Heterogeneous Catalysis

Noritaka Mizuno and Makoto Misono*

Department of Applied Chemistry, Graduate School of Engineering, The University of Tokyo, Hongo, Bunkyo-ku, Tokyo 113, Japan

Received May 3, 1997 (Revised Manuscript Received September 2, 1997)

Contents

I. Characteristics of Heteropoly Compounds for Solid Catalysts

Heteropoly compounds provide a good basis for the molecular design of mixed oxide catalysts and they have high capability in practical uses. This is because the relationships among the following four levels of information can be established on the molecular basis: (i) catalytic performance; (ii) chemical and physical property; (iii) molecular and bulk composition and structure; and (iv) method of synthesis of catalyst. We assume that these relationships are most useful for the design of practical catalysts.[1−5]

The catalytic function of heteropoly compounds has attracted much attention particularly in the last two decades. They are used in solution as well as in the solid state as acid and oxidation catalysts. The reason why heteropoly catalysts are attractive is their variety and high potential as catalyst. The advantageous characteristics are listed in Table 1 (cf. refs 1 and 2 for more detailed information).

Systematic research of heterogeneous catalysis that started in the mid-1970s has disclosed the presence of quantitative relationships between the acid or redox properties and catalytic performance of heteropoly catalysts as well as their unique behavior in heterogeneous catalysis such as pseudoliquid-phase (bulk-type (I)) and the bulk-type (II) catalysis.[1−11]

There are already several industrial processes which utilize heteropoly catalysts.[1,12] Many known and new heteropoly compounds are being applied to a wide variety of reactions. The newest commercial process, the direct oxidation of ethylene to acetic acid catalyzed by palladium plus HPAs, will start by the end of 1997 in Japan (100 000 ton/year). It is evident that the research activity of heteropoly catalysis is very high and still growing.

In this article, we attempted to avoid the overlapping with our previous review,[1] but the minimum fundamental aspects are given to provide a sound overview about the present subject. The term heteropoly compounds (HPAs) is used for the hydrogen (or acid) forms and the salts. HPAs can be utilized for precursors of oxide catalysts, but this will not be included in this review. The present review focuses mostly on the Keggin HPAs, as there have been rather few systematic studies on the heterogeneous catalysis of well-characterized HPAs other than the Keggin HPAs.

II. Structure of Heteropoly Compounds in the Solid State

A. Primary, Secondary, and Tertiary Structures

It is very important, in our view, for understanding the heterogeneous catalysis of HPAs to distinguish

* Corresponding author.

S0009-2665(96)00401-3 CCC: $30.00
Published on Web 01/08/1998

Noritaka Mizuno was born in 1957 in Shizuoka Prefecture of Japan. He received his Bachelor's degree in synthetic chemistry at the University of Tokyo in 1980. Then he started his research on the heterogeneous oxidation catalysis of heteropoly compounds at the University of Tokyo and received his Ph.D. in 1985. He continued the study of heterogeneous catalysis as a research associate at the same place. In 1989 he did a postdoctoral work with Professor Richard G. Finke at University of Oregon. In 1990, he returned to Japan as an Associate Professor at Catalysis Research Center, Hokkaido University. In 1994, he moved to the Institute of Industrial Science, the University of Tokyo, and then to the Department of Applied Chemistry of the same university, where he has been an Associate Professor since 1996. His research interests are mainly directed toward catalysis of metal oxide clusters such as heteropoly compounds and zeolitic materials and their syntheses.

Makoto Misono was born in 1939 in Kagoshima Prefecture of Japan. He received his Bachelor, Master, and Doctor's degrees in Engineering at the University of Tokyo in 1961, 1963, and 1966, respectively. He has been studying heterogeneous catalysis and related materials chemistry over 35 years. His first appointment was a research associate at the University of Tokyo. He spent two years from 1967 as a postdoctorate in the United States, first with Professor P. W. Selwood at University of California, Santa Barbara, and then with Professor W. Keith Hall at Mellon Institute, Pittsburgh, PA. He has been a full professor at the University of Tokyo since 1983. His research interests are the design of catalysts based on well-defined metal oxides such as heteropoly compounds and perovskites, and environmental catalysts like deNOx catalysts. He is ex-President of the Catalysis Society of Japan and presently Vice-President of the Chemical Society of Japan.

between the two classes of structures which we call the primary and the secondary structures.[1,2,4,13] As a reference to the differences, 12-tungstophosphoric acid is shown in Figure 1.[14,15] HPAs in the solid state are ionic crystals (sometimes amorphous) consisting of large polyanions (primary structure), cations, water of crystallization, and other molecules. This

Table 1. Advantage of Solid Heteropoly Catalysts

1. catalyst design at atomic/molecular levels based on
acidic and redox properties, which are controllable
multifunctionality such as acid−redox, acid−base, etc.
controllable tertiary structure and bulk-type behavior
2. molecularity—metal oxide cluster
molecular design of catalysts
cluster models of mixed oxide catalysts
description of catalytic processes at atomic/molecular levels
3. unique reaction field
bulk-type catalysis such as "pseudoliquid"
shape selectivity
4. unique basicity of polyanion
selective stabilization of reaction intermediates
ligands and supports for metals and organometallics

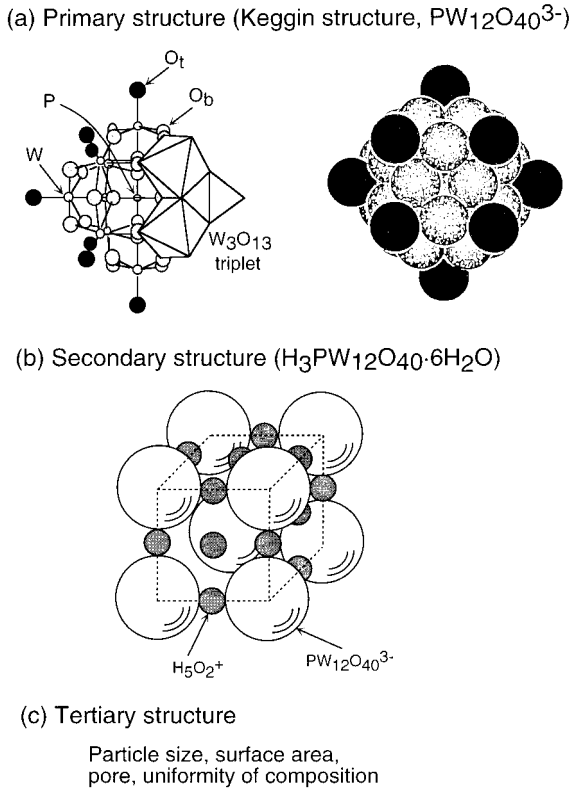

Figure 1. Primary, secondary, and tertiary structures of HPAs: (a) primary structure (Keggin structure, $PW_{12}O_{40}$), (b) secondary structure ($H_3PW_{12}O_{40}\cdot 6H_2O$), and (c) tertiary structure.

three-dimensional arrangement is the "secondary structure".

Recently, it was realized that, in addition to these two structures, the tertiary structure is very influential on the catalytic function of solid HPAs.[1,2] The tertiary structure is the structure of solid HPAs as assembled. The size of the particles, pore structure, distribution of protons in the particle, etc., are the elements of the tertiary structure. Thus, HPAs in the solid bulk have hierarchic structures. Countercations greatly influence the tertiary structure of HPAs, and the salts are classified by the size of cation into group A (small metal ions like Na and Cu) and group B (large metal ions like Cs, NH_4, etc.).[16]

The location of the protons in dehydrated $H_3PW_{12}O_{40}$ is controversial. The IR spectrum of $H_3PW_{12}O_{40}\cdot 6H_2O$ showed broad bands at 2900−3600 and 1500−1800 cm^{-1} due to $\nu(H^+(H_2O)_2)$ and δ (H^+-

$(H_2O)_2$), respectively,[17−20] and both bands disappeared by the evacuation at elevated temperatures.[20] Although there is no reliable explanation for the disappearance by evacuation even at 423 K, it is possible that protons are only weakly bound and mobile, giving a very diffuse band. We observed that there were significant differences in the shifts of the ν(W−O_e−W) bands (O_e, edge-shared oxygen) during the dehydration process of $H_3PW_{12}O_{40}\cdot 6H_2O$ and $D_3PW_{12}O_{40}\cdot 6D_2O$ and indicated that the protons migrate from the terminal oxygen onto the bridging oxygen upon dehydration above 373 K.[21] Kozhevnikov et al. suggested that protons are located at terminal oxygens (hopping around?) on the basis of the 60 ppm upfield shift of the ^{17}O NMR signal of terminal oxygen upon the dehydration of $H_3PW_{12}O_{40}\cdot nH_2O$ at 473 K.[22]

The relative intensities of four ^{31}P NMR peaks for $Cs_xH_{3-x}PW_{12}O_{40}$ ($x = 0-3$) demonstrated that all protons of $Cs_{2.5}H_{0.5}PW_{12}O_{40}$ are distributed nearly uniformly through the solid bulk.[2,23] In other words, they are solid solutions of $H_3PW_{12}O_{40}$ and $Cs_3PW_{12}O_{40}$. In addition, the same ^{31}P NMR spectrum was observed when the sample was prepared by impregnating $H_3PW_{12}O_{40}$ on $Cs_3PW_{12}O_{40}$ to form the same average composition. Hence, it is certain that homogenization proceeds by the migration of Cs ion and proton.[2,23−25] On the other hand, Essayem et al. suggested on the basis of ^{31}P NMR and XRD data, which were prepared in a slightly different way, that hydrogen cesium salt corresponds to $Cs_3PW_{12}O_{40}$ with a highly dispersed $H_3PW_{12}O_{40}$ entrapped in the pores.[26]

In many cases, the primary structure in solution is maintained as confirmed by XRD, IR, Raman, and NMR spectroscopies after solid HPAs are obtained by the evaporation to dryness or by precipitation. Figure 1a shows the $PW_{12}O_{40}^{3-}$ Keggin structure. The preservation of the primary structure in the solid state is shown for most of the other cases, too. There are four different kinds of oxygen. Figure 1b shows the secondary structure of its hydrogen form in hexahydrate state, which was confirmed by neutron diffraction.[27] In this case, the $PW_{12}O_{40}^{3-}$ polyanions are bridged by hydrated protons, $H^+(H_2O)_2$.

The secondary structure is very variable for the group A salts. For example, in the case of $H_3PW_{12}O_{40}\cdot nH_2O$, it is cubic for $n = 0-6$ (lattice constants are 1.17 nm for $n = 0.3$ and 1.213 nm for $n = 6$), and also cubic for $n = 29$ but the lattice constant is 2.333 nm.[27−29] The crystal structures of Cs and NH_4 salts are the same as the cubic $H_3PW_{12}O_{40}\cdot 6H_2O$,[27] with cations at the sites of $H^+(H_2O)_2$ sites. The pyridine molecules (Py) are also paired around proton forming Py−H^+−Py cations in $[(Py)_2H]_3PW_{12}O_{40}$.[30a] Dimethyl sulfoxide (DMSO) molecules also form DMSO−H^+−DMSO cations in $[(DMSO)_2H]_4SiW_{12}O_{40}\cdot$DMSO.[30b] It must be remembered however that Cs or NH_4 salts of $H_4SiW_{12}O_{40}$ form amorphous or cubic structures. Here the cubic structure accommodates only three large monovalent cations at the regular cation sites. For example, $Cs_3HSiW_{12}O_{40}$ forms a stable cubic structure.

B. Surface Area, Pore Structure, and Self-Assembly

Hydrogen forms and group A salts (e.g., Na, Mg), which are prepared from aqueous solutions, have low surface areas (1−15 $m^2\ g^{-1}$), reflecting their high solubility in water. Partial hydrolysis sometimes occurs due to an increase in pH during neutralization and drying processes. On the other hand, the surface areas of group B salts (Cs, NH_4, etc.) are much higher (50−200 $m^2\ g^{-1}$). Very fine particles are instantaneously precipitated when these cations are titrated to aqueous solutions of $H_3PW_{12}O_{40}$ and $H_3PMo_{12}O_{40}$. As described below, the control of pore structure as well as epitaxial assembly is possible for these salts.

The surface areas of $Cs_xH_{4-x}SiW_{12}O_{40}$ were reported to be 9.0, 23, 49, and 83 $m^2\ g^{-1}$ for $x = 0$, 2, 2.5, and 3, respectively,[31] and those of $Cs_xH_{3-x}PW_{12}O_{40}$ 6.0, 1.0, 1.2, 135, and 156 $m^2\ g^{-1}$ for $x = 0$, 1, 2.5, and 3, respectively.[32] Similarly, in the case of $Cs_xH_{4-x}PVMo_{11}O_{40}$, the surface areas were 2.6, 11.2, 10.0, 130, 164, and 103 $m^2\ g^{-1}$ for $x = 0$, 1, 2, 3, 3.5, and 4, respectively.[33] The surface areas are variable depending on the precipitation and drying process. Washing partially removes hydrogen forms in the product.

The pores of HPA described here are interparticle, not intracrystalline, according to the TEM observation and nitrogen adsorption measurement.[34] $Cs_3PW_{12}O_{40}$ is composed of fine primary particles as observed by TEM. Considering the size and shape of the Keggin anion and the crystal structure of $Cs_3PW_{12}O_{40}$, there are no open pores in the crystal structure through which an nitrogen molecule (0.36 nm in diameter) can penetrate. Gregg and Tayyab found that $(NH_4)_3PW_{12}O_{40}$ has micropores (pore diameter; <2 nm).[35] Moffat et al. reported that the salts of NH_4 and Cs possess micro- and mesopores as revealed by nitrogen adsorption and the pore size distribution varies by the size of the cation species.[36] They further suggested that these pores exist in the crystal structure, while we indicated this to be unlikely. Recently, it was found that the micropore structure (>0.59 nm) can be controlled by the partial substitution of H by Cs or NH_4 in $H_3PW_{12}O_{40}$.[37,38]

The pore size of acidic Cs salts ($Cs_xH_{3-x}PW_{12}O_{40}$) was precisely controlled by the Cs content.[24,39,40] Figure 2 shows the adsorption−desorption isotherms of nitrogen. $H_3PW_{12}O_{40}$ exhibited a type II isotherm, indicating that this is nonporous. $Cs_{2.5}H_{0.5}PW_{12}O_{40}$ showed a type IV isotherm, similar to $Cs_3PW_{12}O_{40}$. These have micro- and mesopores.

On the other hand, $Cs_{2.2}H_{0.8}PW_{12}O_{40}$ and $(NH_4)_3PW_{12}O_{40}$ showed a type I isotherm and most of adsorption took place at the very low pressure region, indicating the presence of only micropores. The pore sizes of $Cs_xH_{3-x}PW_{12}O_{40}$ estimated from the adsorption of molecules having various molecular sizes were in the range 0.62−0.72 nm for $x = 2.2$, larger than 0.85 nm for $x = 2.5$, and less than 0.59 nm for $x = 2.1$.[24,39,40]

Probable preparation processes for $Cs_xH_{3-x}PW_{12}O_{40}$ (randomly oriented nanocrystallites formed by precipitation at 298 K) are schematically illustrated in Figure 3.[41] When the Cs content, x, is low, ultrafine

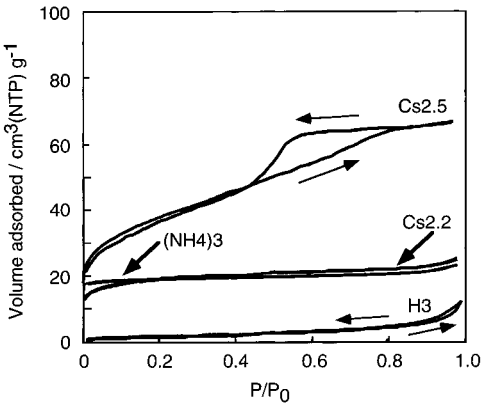

Figure 2. Isotherms of N_2 adsorption on $Cs_xH_{3-x}PW_{12}O_{40}$ and $(NH_4)_3PW_{12}O_{40}$ at 77 K. The catalysts were pretreated at 573 K in vacuum: (→) adsorption branch; (←) desorption branch. $(NH_4)_3PW_{12}O_{40}$ was precipitated at 368 K. H3, Csx, and (NH4)3 denote $H_3PW_{12}O_{40}$, $Cs_xH_{3-x}PW_{12}O_{40}$, and $(NH_4)_3PW_{12}O_{40}$, respectively.

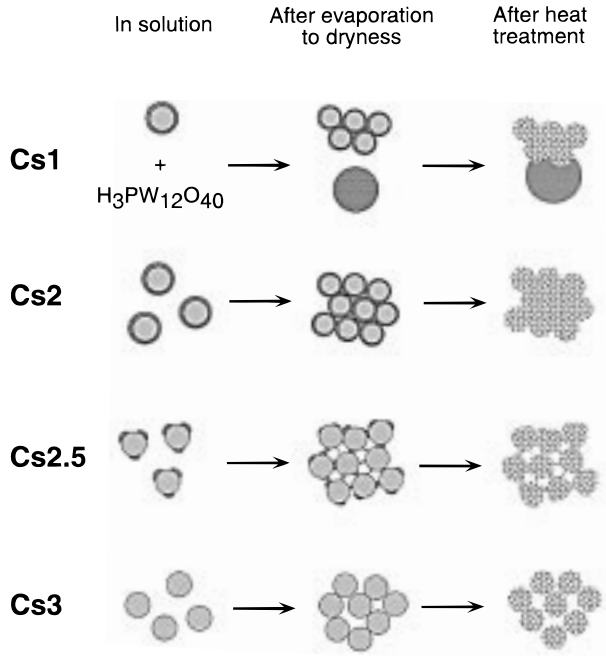

Figure 3. Illustration of the preparation of $Cs_xH_{3-x}PW_{12}O_{40}$: (solid) $H_3PW_{12}O_{40}$; (gray) $Cs_3PW_{12}O_{40}$; (dotted) particles with uniform composition.

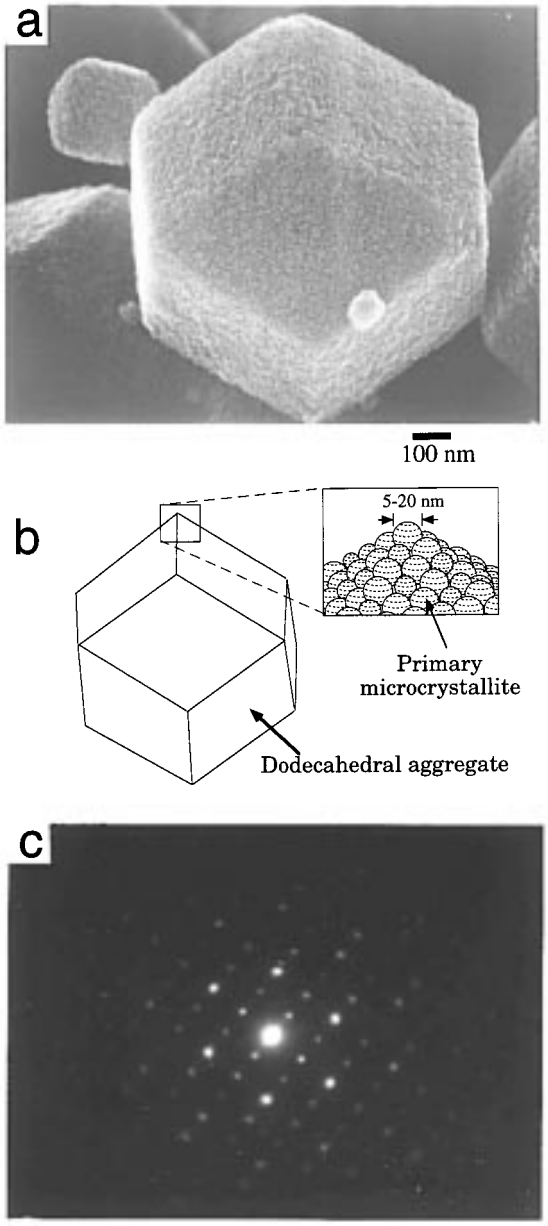

Figure 4. The microstructure of $(NH_4)_3PW_{12}O_{40}$ dodecahedron: (a) SEM image of $(NH_4)_3PW_{12}O_{40}$ prepared at 368 K using $(NH_4)_2CO_3$; (b) schematic illustration of dodecahedron shown in the SEM image; and (c) electron diffraction image.

particles of $Cs_3PW_{12}O_{40}$ (8−10 nm in diameter) are thickly covered by $H_3PW_{12}O_{40}$ after drying the solution. Heat treatment converted them to particles having a size similar to that before heat treatment and nearly uniform composition. This homogenization process was confirmed by ^{31}P NMR and XRD.[23,24] At $x = 2.5$, the hydrogen form, which remains in solution in a small quantity, forms very thin films or small islands on $Cs_3PW_{12}O_{40}$ after drying. Heat treatment produces fine particles having a uniform composition of $Cs_{2.5}H_{0.5}PW_{12}O_{40}$ as discussed in section II.A. This mechanism can explain the unusual trend that the pore size increases with the surface area for $x = 2-3$.

Novel porous aggregates of $(NH_4)_3PW_{12}O_{40}$ and $Cs_3PW_{12}O_{40}$ nanocrystallites are formed by controlling the preparation conditions.[38] Figure 4a shows a SEM image of the aggregate of $(NH_4)_3PW_{12}O_{40}$ precipitated at 368 K. The BET surface area was 78 $m^2\ g^{-1}$, which is much greater than the outer surface of the dodecahedron seen in Figure 4a ($\leq 3\ m^2\ g^{-1}$), demonstrating that the dodecahedron is porous inside. This dodecahedron can be regarded as a single crystal, as discussed below.

The sizes of nanocrystallites in the aggregates were calculated from the BET surface area assuming spherical shape (denoted by d(BET)) and the lengths of ordered crystal structure from the calibrated line width of XRD (denoted by L(XRD)). For dispersed primary particles as in the case of $Cs_3PW_{12}O_{40}$ prepared at 298 K (∼10−15 nm) these two values were comparable with each other. The crystal orientation was random and ring patterns were observed in electron diffraction.

However, for the sample shown in Figure 4a, the L(XRD) and d(BET) were 81−150 nm and 16 nm, respectively. The much larger value of L(XRD) (>80 nm) means that the nanocrystallites (∼16 nm) are connected epitaxially in an aggregate. This is supported by the discrete regular spots observed in electron diffraction as shown in Figure 3c. Hence, the crystal planes of the nanocrystallites orient regularly in an aggregate. In another word, this aggregate looks like a porous single crystal. There is an intermediate case as well; round porous aggregates formed for $(NH_4)_3PW_{12}O_{40}$ precipitated at 273 K and $Cs_3PW_{12}O_{40}$ at 368 K showed regular spots in electron diffraction, but XRD indicates that the epitaxial connections are not well developed.[42] It seems that the solubility of the salts at the precipitation temperature controls the microstructure. The higher the solubility, the more the epitaxial connection between nanocrystallites is formed.

C. Thermal Stability

There are various kinds of stabilities, for example, thermal stability and hydrolytic stability in solution, and those stabilities change very much depending on the kind of HPAs.[1,5] Some solid HPAs are thermally stable and applicable to vapor-phase reactions conducted at high temperatures. The thermal stability of hydrogen forms of HPAs changes with heteroatom, polyatom, and polyanion structure as follows: $H_3PW_{12}O_{40}$ > $H_3PMo_{12}O_{40}$ > $H_4SiMo_{12}O_{40}$, and $H_3PW_{12}O_{40}$ is much more stable than $H_6P_2W_{18}O_{62}$.[43−45] ^{31}P NMR and thermoanalysis indicate that thermolysis of $H_3PMo_{12}O_{40}$ proceeds by losses of water of crystallization and subsequently constitutional water to form $PMo_{12}O_{38.5}$.[46] The presence of $PMo_{12}O_{38.5}$ has not yet been confirmed in the pure state. Above 723 K, the Keggin structure of $H_3PMo_{12}O_{40}$ is completely destroyed.

Thermal stability of mixed-addenda heteropolyanions is low in general. Recently, it has been demonstrated by IR and NMR spectroscopy that V^{5+} in $H_{3+x}PM_{12-x}V_xO_{40}$ (M = Mo, W) is expelled from the polyanion framework upon thermal treatment above 463 K or during catalytic oxidation. In the latter case, the formation of VO^{2+} salt of $H_3PM_{12}O_{40}$ is suggested: $4H^+ + PMo_{11}VO_{40}^{4-}$ + isobutyric acid → $VO^{2+} + 2H^+ + {}^{11}/_{12}PMo_{12}O_{40}^{4.09-} + {}^{1}/_{12}PO_4^{3-} + 2H_2O$ + methacrylic acid.[47,48] On the other hand, it should be considered at the same time that the regeneration of $H_3PM_{12}O_{40}$ from the decomposed mixture sometimes takes place.[49,50]

The thermal stability of $H_3PMo_{12}O_{40}$ and its salts changes with countercations. Bi- and tervalent metal salts are not stable. The hydrogen form and ammonium salt decomposed at 693 and 743 K, respectively. Cs and K salts are stable up to their melting points.[51] The thermal stability changes generally in the order of Ba^{2+}, Co^{2+} < Cu^{2+}, Ni^{2+} < H^+, Cd^{2+} < Ca^{2+}, Mn^{2+} < Mg^{2+} < La^{3+},Ce^{3+} < NH_4^+ < K^+, Tl^+, Cs^+.[51] The thermal stability of Dawson heteropolyanion is also increased by the formation of K salt. $H_6P_2W_{18}O_{62}$ decomposed at 573 K, but the potassium salt was stable at 723 K.[52,53] As for the hydrogen cesium salts, the formation of water by the reaction between proton and the oxide ion in $Cs_{2.5}H_{0.5}PW_{12}O_{40}$ at and above 623 K was recently reported.[54]

D. Adsorption and Absorption Properties

One of the remarkable characteristics is that some solid HPAs (group A, hydrogen forms included) absorb easily a large quantity of polar or basic molecules such as alcohols and nitrogen bases in the solid bulk.[4,18,55] The absorption depends on basicity and the size of the molecule to be absorbed and the rigidness of the secondary structure. As for the desorption, alcohols absorbed can readily leave the bulk, but the desorption of pyridine and ammonia needs a high temperature. Nonpolar molecules like hydrocarbons are usually adsorbed only on the surface of group A and B salts. However, it was suggested that isobutylene was absorbed into HPAs, being assisted by coexisting methanol.[52]

Diffusion coefficients measured quantitatively for $H_3PW_{12}O_{40}$ are much lower than those in the micropores of zeolites but are close to those in the liquid phase.[18,55,56] The quantity of absorbed molecules tends to be integral multiples of the number of protons.[18,55] An interesting application of this behavior is to control the tertiary structure by utilizing pyridinium salts in the preparation of commercial catalysts for the oxidation of methacrolein.[57,58] The rigidness of HPAs depends on the countercations (size, charge, etc.) and apparently on the water content, as well. Group B salts like $Cs_xH_{3-x}PW_{12}O_{40}$ (x > 2) adsorb even polar molecules only on the surface.

IR and NMR spectroscopies provide information about the structure of absorbed species.[21,59−62] For example, the IR spectrum of protonated diethyl ether dimer in $H_3PW_{12}O_{40}$, $[(C_2H_5)_2O-H^+-O(C_2H_5)_2]$, showed a characteristic ν(OH) band at 1527 cm^{-1}.[32] $H_3PW_{12}O_{40}\cdot 6C_2H_5OH$ gave three ^{1}H NMR resonances at 9.5, 4.2, and 1.6 ppm due to OH, CH_2, and CH_3, respectively. This is assigned to a protonated dimer, $(C_2H_5OH)_2H^+$. The chemical shift of the hydroxyl proton of $H_3PW_{12}O_{40}\cdot 6C_2H_5OH$ (9.4 ppm) is close to those reported for protonated ethanol in superacids: 8.3 in $HF-BF_3$, 9.3 in $FSO_3F-SbF_5-SO_2$, and 9.9 ppm in HSO_3F[63] (as compared with 1.0 ppm for a dilute ethanol solution). In this respect, the pseudoliquid phase of $H_3PW_{12}O_{40}$ may be regarded to be a superacidic media. The ^{13}C NMR spectrum demonstrates the presence of three different species for ethanol absorption: $(C_2H_5OH)_2H^+$, $C_2H_5OH_2^+$, and ethoxide in $H_3PW_{12}O_{40}$.

The dynamic behavior of CH_3OH molecules in the pseudoliquid phase has been analyzed in detail.[61] Figure 5 shows ^{1}H NMR spectra of $H_3PW_{12}O_{40}\cdot n^{13}CH_3OH$ with n = 1, 6, 7, and 9. For n = 0, a broad peak was observed at 10.0 ppm (not shown). The peak at around 5 ppm is due to the methyl group of $^{13}CH_3OH$. Besides this methyl proton, one peak was observed at 9−11 ppm for all samples. This is assigned to the coalesced peak of hydroxyl protons of $^{13}CH_3OH$ and acidic protons of $H_3PW_{12}O_{40}$. This indicates that these protons are mobile and exchanging the positions rapidly with each other. The line width (Figure 5) exhibited drastic narrowing for both

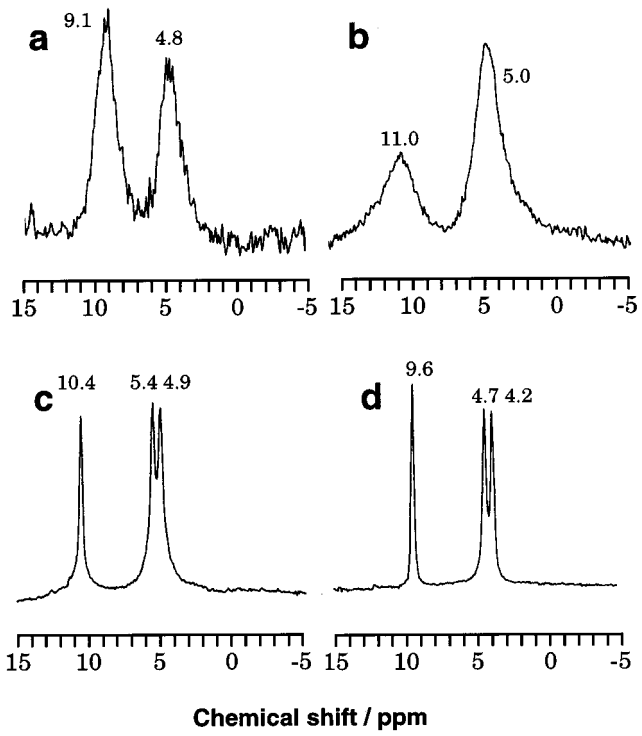

Figure 5. ^{1}H MAS NMR of $^{13}CH_3OH$ absorbed in $H_3PW_{12}O_{40}$. The molar ratio of $^{13}CH_3OH$ to $H_3PW_{12}O_{40}$ is (a) 1, (b) 6, (c) 7, and (d) 9.

methyl and hydroxyl peaks when *n* exceeded 6. Thus, the hydroxyl protons of CH_3OH and the protons of $H_3PW_{12}O_{40}$ exchange rapidly in a wide range of absorption level, but CH_3OH molecules become very mobile when *n* exceeded 6.

It was reported that $H_3PW_{12}O_{40}$ absorbed NO up to 3 molecules/anion. The heating of the NO-containing $H_3PW_{12}O_{40}$ produced nitrogen,[64,65] although the structural changes have not been elucidated.

E. Supported HPAs

Dispersing HPAs on solid supports with high surface areas is important for catalytic application because the surface area of unsupported HPAs are usually low ($1-10\ m^2\ g^{-1}$). The supported catalysts are characterized by various methods and the changes in the acid strength, redox properties, and structure have been reported. In general, HPAs strongly interact with supports at low loading levels, while the bulk properties of HPAs prevail at high loading levels. Acidic or neutral substances such as SiO_2, active carbon, acidic ion-exchange resin are suitable supports, the most frequently used support being SiO_2.[1,2,4] Solids having basicity such as Al_2O_3 and MgO tend to decompose HPAs (note the pH range of hydrolysis of heteropolyanion).[66-69]

Certain active carbons can firmly entrap HPAs and, therefore, show high stability against the leakage into solvent from the carrier, when HPAs are used in solution.[70-72] The maximum loading level of HPAs on carbons was 7−14 wt % and varied moderately with the physical properties of the carbon support, but little with the chemical treatment.[8]

Enhanced catalytic activity of HPAs was found when they were supported on a strongly acidic ion-exchange resin, Amberlyst-15.[73,74] The activity was much higher than those of Amberlyst-15 and of the acids supported on active carbon. The higher activity was explained by the synergism due to the interaction of the heteropolyanions and protons of the ion exchanger.

It has been reported that $H_3PMo_{12}O_{40}$ was uniformly and finely immobilized into a polysulfone film. The catalyst exhibited an improved catalytic activity for the conversion of alcohols such as ethyl and isopropyl alcohol.[75,76] For example, this film catalyst showed a higher yield of acetone but a lower yield of propene than $H_3PMo_{12}O_{40}$ itself. This is mainly because the acidic function of $H_3PMo_{12}O_{40}$ is suppressed by the adsorbed dimethyformamide and the formation of acetone is enhanced by the uniformly and finely dispersed $H_3PMo_{12}O_{40}$ in polysulfone film.[75]

Microcalorimetry of ammonia absorption (adsorption) reveals that the supporting of $H_3PW_{12}O_{40}$ on to SiO_2 results in a decrease in the acid strength. Only 20% of the entire protons remained as strong as those in the neat $H_3PW_{12}O_{40}$, and the rest showed heats of adsorption similar to those of HX and HY zeolites.[71] It was reported that the acid strength of supported $H_3PW_{12}O_{40}$ diminishes in the sequence of supports: $SiO_2 > \alpha\text{-}Al_2O_3 >$ activated charcoal.[77] The interactions between $H_3PW_{12}O_{40}$ and the surface OH groups of SiO_2 have been detected at low loading levels by ^{1}H and ^{31}P MAS NMR and Raman spectroscopies.[78-82]

SiO_2-supported heteropolymolybdates such as $H_4SiMo_{12}O_{40}$, $H_3PMo_{12}O_{40}$, and $H_5PMo_{10}V_2O_{40}$ retain mostly the Keggin structure at a high loading level, but partly decompose at very low loading due to their strong interactions with surface silanol groups.[83-88] It is notable that a thermally decomposed Keggin structure on SiO_2 surface can be reconstructed in some cases upon exposure to water vapor.[83,89] It was also reported for a SiO_2 support that P in $H_3PW_{12}O_{40}$ is partially replaced with Si of the support.[90] Thus, heteropolyanions on the oxide surface show dynamic behavior depending on the conditions.

Recently, $H_3PW_{12}O_{40}$ supported on mesoporous pure-silica molecular sieve MCM-41 and pillared layered double hydroxide exchanged with Keggin heteropolyanions have been reported.[91] It is claimed in the former case that $H_3PW_{12}O_{40}$ retains the Keggin structure at loading levels above 20 wt %. No crystalline phase of $H_3PW_{12}O_{40}$ is seen at loading levels as high as 50 wt % (see later section for catalytic function). The acid catalysis by micro- or mesoporous $Cs_xH_{3-x}PW_{12}O_{40}$ ($x \geq 2.1$) will be described also in the later section.

III. Acid and Redox Properties

A. Acidic Properties

In early studies, it was shown that HPAs such as $H_3PW_{12}O_{40}$ and $H_3PMo_{12}O_{40}$ in the solid state are pure Brønsted acids[92] and stronger acids than the conventional solid acids such as SiO_2-Al_2O_3, H_3PO_4/SiO_2, and HX and HY zeolites.[77,93] According to an indicator test using Hammett indicators, $H_3PW_{12}O_{40}$ was suggested to be a superacid,[93-96] but firm evidence has not been obtained. Although pyridine

adsorbed on SiO_2-Al_2O_3 is completely desorbed at 573 K, pyridine sorbed in $H_3PW_{12}O_{40}$ mostly remains at 573 K, indicating that $H_3PW_{12}O_{40}$ is a very strong acid.[18] Here, it is to be noted that the interaction energy between HPAs and pyridine contains somehow the lattice energy of the pyridinium salt.

Thermal desorption of ammonia also shows that $H_3PW_{12}O_{40}$ is an acid stronger than ZSM-5, but weaker than SO_4^{2-}/ZrO_2.[94] Here nitrogen was also formed from ammonia, so that it was assumed that the nitrogen formation from ammonia took place after ammonia desorption. The strengths of heteropolytungstic acids have recently been determined more quantitatively by calorimetry of ammonia absorption.[77,97] Since the ammonia uptake takes place in the solid bulk, the contribution from the heat of lattice formation is included in these values as in the case of pyridine. The data show that the acid sites of $H_3PW_{12}O_{40}$ are rather uniform and more strongly acidic than those of H-ZSM-5. The initial heats of absorption of ammonia measured at 423 K were 196, 185, 164, and 156 kJ mol^{-1} for $H_3PW_{12}O_{40}$, $H_4SiW_{12}O_{40}$, $H_6P_2W_{21}O_{71}(H_2O)_3$, and $H_6P_2W_{18}O_{62}$, respectively.[77] The Keggin HPAs are much stronger acids than Dawson HPAs. The heats of ammonia adsorption were 150 and 140 kJ mol^{-1} for HZSM-5 and γ-Al_2O_3, respectively.[97] Recently, it has been indicated by the calorimetric titration in acetonitrile that anhydrous $H_3PW_{12}O_{40}$ is a superacid.[98]

The strength and the number of acid centers of HPAs can be controlled by the structure and composition of heteropolyanions, the extent of hydration, the type of support, the thermal pretreatment, etc.

The acidic properties of salts are more complex. Five mechanisms have been proposed for the generation acidity in metal salts:[1,4] (i) dissociation of coordinated water, for example refs 1 and 5, $Ni(H_2O)_m^{2+} \rightarrow Ni(H_2O)_{m-1}(OH)^+ + H^+$; (ii) Lewis acidity of metal ions; (iii) protons formed by the reduction of metal ions, $Ag^+ + {}^1/_2H_2 \rightarrow Ag^0 + H^+$; (iv) protons present in the acidic salts, for example, e.g., $Cs_xH_{3-x}PW_{12}O_{40}$; (v) partial hydrolysis during the preparation process, for example, $H_3PW_{12}O_{40} + 3H_2O \rightarrow PW_{11}O_{39}^{7-} + WO_4^{2-} + 9H^+$.

Many efforts are still being devoted to characterize the acidity of the salts of HPAs, by means of adsorption and thermal desorption of basic molecules[77] as well as by NMR.[98−102]

The temperature programmed desorption (TPD) of ammonia showed that $Cs_{2.5}H_{0.5}PW_{12}O_{40}$ and $H_3PW_{12}O_{40}$ have similar acid strength.[21] According to indicator tests, $Cs_{2.5}H_{0.5}PW_{12}O_{40}$ like $H_3PW_{12}O_{40}$ had the acid strength ≤ -13.16.[21] In TPD of ammonia, $Cs_{2.5}H_{0.5}PW_{12}O_{40}$ gave a little broader peak than $H_3PW_{12}O_{40}$, showing a slight inhomogeneiety of the acid strength.[94] As the Cs content, x in $Cs_xH_{3-x}PW_{12}O_{40}$, increased, the number of surface protons decreased at first, but greatly increased when the Cs content exceeded 2 and showed the highest surface acidity at $x = 2.5$ (see below for interpretation).[23]

Protons are formed by the reduction of Ag^+ in $Ag_3PW_{12}O_{40}$ (type iii).[98−102] $Ag_3PW_{12}O_{40}$ generated two kinds of protons, at 6.4 and 9.3 ppm in H-NMR, when the silver salt was partially reduced with hydrogen.[99,102] The former appeared only when hydrogen was present in the gas phase. The dependence of the line shapes of the two peaks on the spinning rate indicated that the protons observed at 6.4 ppm are mobile even at room temperature, while the protons observed at 9.3 ppm are not. When the temperature was raised to 373 K in the presence of hydrogen, they merged into one peak, due to the exchange between the two kinds of protons. On the other hand, the temperature dependence of the line width was not observed for $H_3PW_{12}O_{40}$ (9.1 ppm).

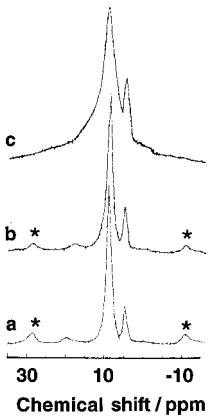

Figure 6. Temperature dependency of ^1H MAS NMR spectrum of Pd^0-$H_3PW_{12}O_{40}$ in the presence of hydrogen: (a) 298 K, (b) 333 K, and (c) 373 K. Conditions: spinning rate, 5.8 kHz; resonance frequency, 300 MHz. The asterisks (*) show the spinning side bands.

It was reported for Pd^0-$H_3PW_{12}O_{40}$ that the hydrogen atoms spillover to the surrounding heteropolyanions: H on $Pd^0 \rightleftharpoons H^+$ in $H_3PW_{12}O_{40}$.[103] As shown in Figure 6a, hydrogen atoms adsorbed on Pd^0 and protons in $H_3PW_{12}O_{40}$ were observed at 19.8 and 9.1 ppm, respectively. The peak at 4.7 ppm is attributed to H_2O molecules. When Pd^0-$H_3PW_{12}O_{40}$ catalyst was heated to 333 K in the presence of hydrogen, the line widths of two peaks at 19.8 and 9.1 ppm were broadened and the peak of hydrogen atoms shifted toward that of acidic protons at 9.1 ppm (Figure 6b,c). This indicates that the interconversion occurs between them and that the hydrogen atoms on Pd^0 spillover to the surrounding polyanions. The line width of the peak at 9.1 ppm depended on the spinning rate at 373 K, indicating that the protons are mobile. The fact is in contrast with the independence of the peak on the spinning rate in the case of $H_3PW_{12}O_{40}$ at 373 K.

B. Redox Properties

The oxidizing ability of HPAs in the solid state has been estimated by various methods: rates of reduction of HPAs,[13,104−110] and ESR and XPS spectra of reduced HPAs.[16,49,111−115] It must be considered that the results are affected significantly by the method of reduction as well as the purity of the samples.[1,4] Another important reason for the apparent inconsistency in the literature may be the ignorance of the presence of surface- and bulk-type reactions (see below).

Various parameters such as the heat of oxide formation, ionic potential, the electronegativity, etc.,

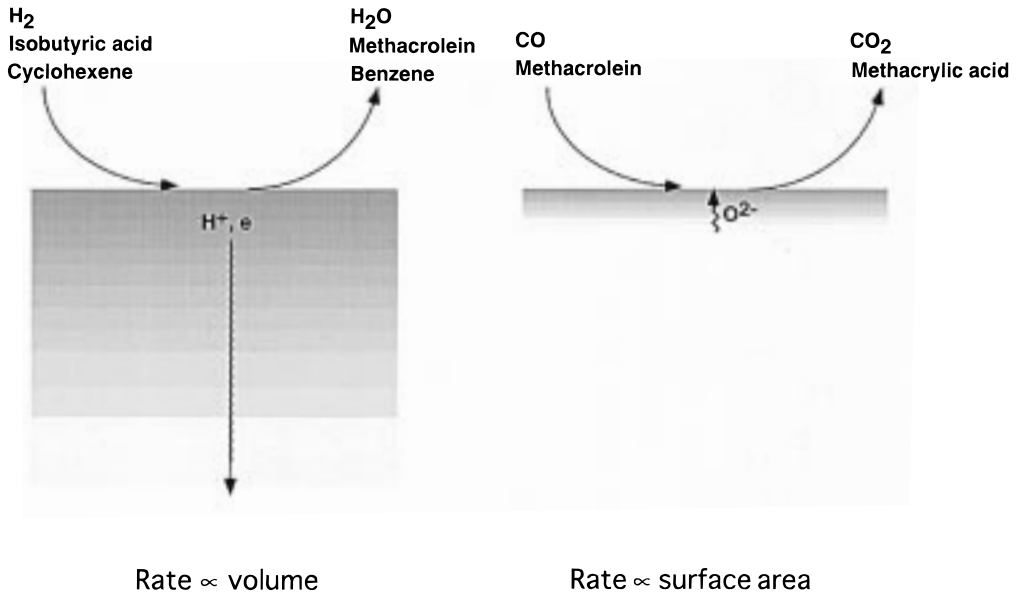

Figure 7. Schematic illustration of bulk-type (II) and surface-type catalysis: (a) bulk type and (b) surface type.

have been proposed for the controlling factors of the redox property.[116−118] As to the controlling methods, the selection of the kinds of cation and the polyanion composition have been investigated. Although clear correlations have not been attained yet, several useful trends have been pointed out.[1,4]

1. Reduction Mechanism

The reduction of $H_3PM_{12}O_{40}$ (M = Mo, W) and its Na salts by hydrogen proceeds in the following three steps:[13,104,105,119]

$$x\mathrm{H_2}\ (\mathrm{gas}) + \underset{\mathrm{I}}{\mathrm{PM_{12}O_{40}}^{3-}}\ (\mathrm{surface}) \rightleftharpoons 2x\mathrm{H^+}\ (\mathrm{bulk}) + \underset{\mathrm{II}}{\mathrm{PM_{12}O_{40}}^{(3+2x)-}}\ (\mathrm{bulk}) \quad (1)$$

$$2x\mathrm{H^+}\ (\mathrm{bulk}) + \underset{\mathrm{II}}{\mathrm{PM_{12}O_{40}}^{(3+2x)-}}\ (\mathrm{bulk}) \rightarrow \underset{\mathrm{III}}{\mathrm{PM_{12}O_{40-x}}^{3-}}\ (\mathrm{bulk}) + x\mathrm{H_2O}\ (\mathrm{bulk}) \quad (2)$$

$$x\mathrm{H_2O}\ (\mathrm{bulk}) \rightarrow x\mathrm{H_2O}\ (\mathrm{gas}) \quad (3)$$

The first step is $H_2 \rightarrow 2H^+$ (present between polyanions) + 2e (present in polyanion), without formation of water. Here the number of electrons introduced per anion is variable. In the second step, the protons formed in the first step react with the oxygen of polyanion to form water, which evolves in step 3 into the gas phase.[20,104] Further reduction brings about irreversible reduction to several species.

As far as the Keggin structure is maintained during reduction (I → II), most of Mo^{5+} are not detectable by ESR due to the rapid electron hopping as in solution.[120] A heat treatment converts II to III, and the Mo^{5+} signal grows, electrons being localized. IR studies on isotopic oxygen exchange and the reduction process indicate that reactive oxygen is the bridging oxygen.[111,112,121] A quantum chemical calculation by Xα method is consistent with this idea.[122]

The diffusion of protons and electrons in the solid of $H_3PM_{12}O_{40}$ (M = Mo, W) is very rapid as compared with the rate of reduction,[119,123] since the isotopic equilibration of H_2-D_2 in the gas phase as well as in the entire solid phase was very rapid (573 K). Electronic conductivity measurements (electron as well as proton) at 473−523 K supported this, while the conductivity very much depended on the composition and thermal treatment.[124] At low temperatures the proton conduction prevails.[125] The detailed kinetic analysis shows that eq 1 is very rapid and eq 2 is the slow step: I ⇌ II → (slow) III. With $H_3PW_{12}O_{40}$, the equilibrium strongly favors the left side of eq 1, while for $H_3PMo_{12}O_{40}$ the equilibrium favors the right side.[119,123]

Since the reduction of $H_3PM_{12}O_{40}$ (M = Mo, W) by hydrogen proceeds in the solid bulk by the rapid migration of protons and electrons,[119,123,126] the rate depends little on the specific surface area. In other words, the rate is proportional to the number of polyanions in the bulk.

In contrast, the rates of reduction by CO of $H_3PMo_{12}O_{40}$ and its alkali salts under the dry conditions are proportional to the specific surface areas as in the case of ordinary heterogeneous catalysis (surface type). Hence, due to the slow diffusion of oxide ion, the reduction mostly proceeds near the surface.[110] The slow diffusion of oxide ion is demonstrated by the effect of the interruption[105] of the reoxidation by oxygen on its time course and the relative rates of isotopic exchange for $^{16}O_2$-$^{18}O_2$-$H_3PMo_{12}O_{40}$ and $H_2{}^{18}O$-$H_3PMo_{12}O_{40}$.[127]

The contrast between the two types is found in organic reactions, as well. The noncatalytic reduction of $H_3PMo_{12}O_{40}$ by the dehydrogenation of isobutyric acid or cyclohexene belongs to the bulk type (II) (Figure 7a) and the reduction by the oxygenation of methacrolein or acetaldehyde belongs to the surface type (Figure 7b). Catalytic reactions of the two types will be described in the later section.

Table 2. Three Types of Heterogeneous Catalysis of HPA

types	remarks	examples
surface type	ordinary type reactions take place on the surface rate ∝ surface area	oxidation of aldehydes and CO
bulk type (I)	"pseudoliquid phase" reactants are absorbed in solid bulk and react rate ∝ volume (weight)	dehydration of alcohols at low temperatures
bulk type (II)	main reactions occur on the surface, but by diffusion of redox carriers, whole bulk takes part rate ∝ volume (weight)	oxidative dehydrogenation and oxidation of H_2

2. Reoxidation

In general, when the extent of reduction is low, the reoxidation is fast and reversible. In the case of $H_3PMo_{12}O_{40}$,the redox cycle between I ⇌ II is rapid and reversible; I ⇌ III, rapid near the surface, but slow in the bulk, and both reversible; and I ⇌ III′ (excessively reduced species), slow and mostly irreversible (I, II, and III refer to eqs 1−3).[105]

In the reoxidation by oxygen of one-electron (1 e) reduced $Cs_xH_{3-x}PMo_{12}O_{40}$, the rates divided by the surface area show a monotonic variation with x, indicating surface-type behavior.[1,105b] A similar variation was observed for Na and K salts. It was suggested that the reoxidizability increases with an increase in the standard electrode potential of the countercation.[128] The presence of water vapor sometimes accelerates the migration of oxide ion, probably in the form of OH^- or H_2O and makes surface-type reactions more like bulk type (II).[110]

It was reported in solution that oxidation of $P_2W_{18}O_{62}^{7-}$ and $PV_2Mo_{10}O_{40}^{7-}$ proceeds by 7-coordinate metal centers with M−O bond, such as bridging and terminal oxygen adducts or ozonide.[129−131] Very recently, it was also reported by ^{17}O NMR experiments in solution that the reoxidation of II → I proceeds by an outer-sphere mechanism without participation of lattice oxide ions.[129] This mechanism appears more probable since the energetics of the sterically congested metal centers and the weak O−O bond in an ozonide are unattractive and the rates of II → I, at least in some systems, are known to be faster than that of oxygen exchange between H_2O and polyanions.[132−135] It is interesting to study how the reoxidation mechanism in solution reflects on that in the solid state.

3. Effects of Constituent Elements on the Redox Properties

The effect of mixed-addenda atoms is important to control the redox properties, as mixed-addenda HPAs are utilized as industrial oxidation catalysts. However, the redox mechanism and its relation to oxidation catalysis remain unclarified. For example, the rate of reduction by hydrogen is slower and less reversible for solid $PMo_{12-x}V_xO_{40}^{(3+x)-}$ than for solid $PMo_{12}O_{40}^{3-}$ although in solution the former systems are stronger oxidants than the latter.[136] The thermal treatment of $H_4PMo_{11}VO_{40}$ formed $PMo_{12}O_{40}^{3-}$ and VO^{2+} and the reduction of $H_4PMo_{11}VO_{40}$ with isobutyric acid formed $PMo_{12}O_{40}^{4.09-}$, VO^{2+}, PO_4^{3-}, and methacrylic acid.[47,48] These decomposition reactions are deeply related to the controversy about the effects of substitution by V for Mo on the catalytic activity.[47,48,136−140] It is also unclear why the rate of reduction decreases with the content of alkali cation.[105]

IV. Heterogeneous Catalysis

A. Three Types of Catalysis

There are three types of catalysis of solid HPAs; (1) surface, (2) bulk type I (= pseudoliquid), and (3) bulk type II catalysis, as shown in Table 2. The latter two were demonstrated so far specifically for heteropoly catalysts, but could be found for other solid catalysts, as well.

1. Surface-Type Catalysis

Surface-type catalysis is the ordinary heterogeneous catalysis, where the reactions take place on the two-dimensional surface (outer surface and pore wall) of solid catalysts. The reaction rate is proportional to the surface area in principle. Rates of double-bond isomerization of olefins are proportional to the surface area of $H_3PMo_{12}O_{40}$.[141] Most acid-catalyzed reactions over $Cs_xH_{3-x}PW_{12}O_{40}$ ($2 < x < 3$) show similar parallelism between the rate and surface acidity.[1,2]

2. Bulk-Type (I) Catalysis

In the bulk-type (I) catalysis, e.g., acid-catalyzed reactions of polar molecules over the hydrogen forms and group A salts at relatively low temperatures, the reactant molecules are absorbed in the interpolyanion space of the ionic crystal (not intrapolyanion) and react there, and then the products desorb from the solid.[5,18,55] The solid behaves in a sense like a solution and the reaction field becomes three dimensional. Therefore, we call this "pseudoliquid" catalysis. The reaction rate is proportional to the volume of catalyst in the ideal case, or, for example, the rate of acid-catalyzed reaction is governed by the bulk acidity. This type of catalysis has been observed not only for gas−solid but also for liquid−solid systems.[142]

The transient response method by using deuterated and nondeuterated alcohols confirmed that a large number of alcohol molecules are absorbed in the catalyst bulk under the reaction conditions of dehydration and the adsorption/desorption is faster than the dehydration.[143]

The unusual pressure dependencies of the rate and selectivity associated with the pseudoliquid were

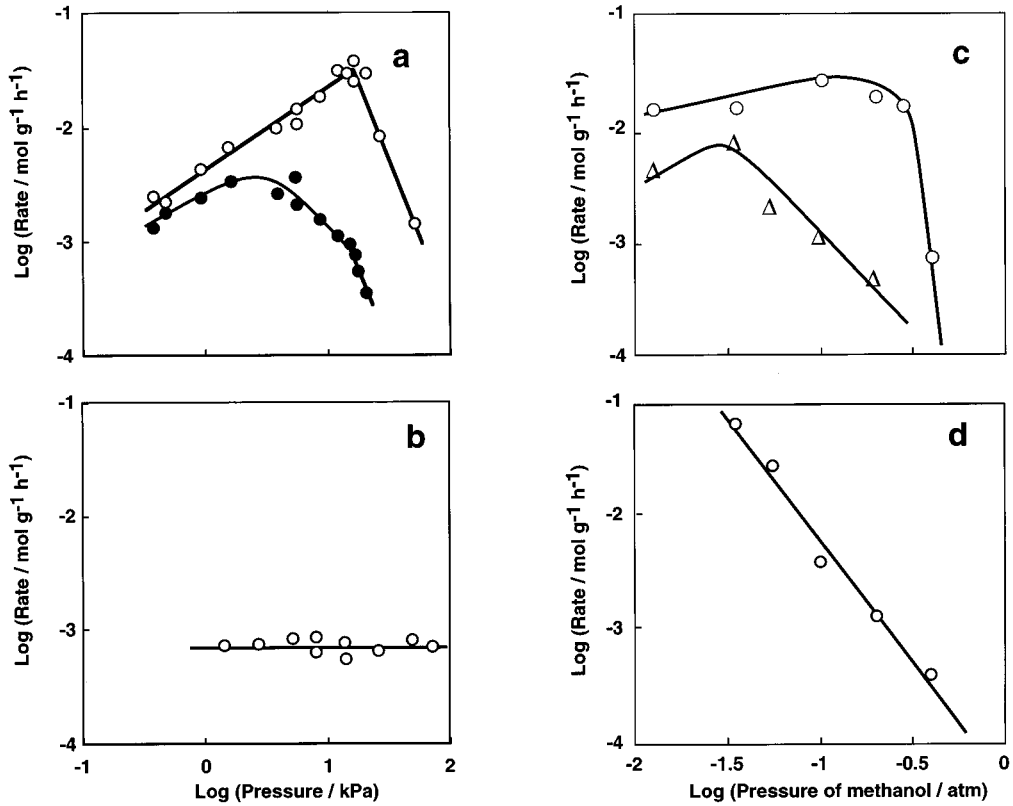

Figure 8. Rates of formation of diethyl ether and ethylene from ethanol and those of formation of MTBE from isobutylene and methanol catalyzed by $H_3PW_{12}O_{40}$ and $Cs_{2.5}H_{0.5}PW_{12}O_{40}$ as a function of the partial pressure of ethanol and methanol: (a and b) formation of diethyl ether (○) and ethylene (●) at 403 K; (c and d) formation of MTBE at 323 K; (a) $H_3PW_{12}O_{40}$; (b) $Cs_{2.5}H_{0.5}PW_{12}O_{40}$; (c) $H_3PW_{12}O_{40}$ (△) and $H_6P_2W_{18}O_{62}$ (○); and (d) $Cs_{2.5}H_{0.5}PW_{12}O_{40}$.

observed for alcohol dehydration,[59,144,145] etherification,[59,144,145] and methyl *tert*-butyl ether (MTBE) synthesis.[47] Examples are shown in Figure 8;[144,145] hydrogen forms exhibit unusual pressure dependencies in contrast to the surface-type catalysis of $Cs_{2.5}H_{0.5}PW_{12}O_{40}$. In the case of the dehydration of ethanol, the amounts of ethanol absorbed under the reaction conditions corresponded to 4−80 times the monolayer value and the change in the amount corresponded to the unusual pressure dependency of the reaction.[59] It is notable that the activity of $H_3PW_{12}O_{40}$ is 10^2 times greater than that of SiO_2-Al_2O_3.[146]

Scheme 1. Reaction Scheme for Dehydration of Ethanol

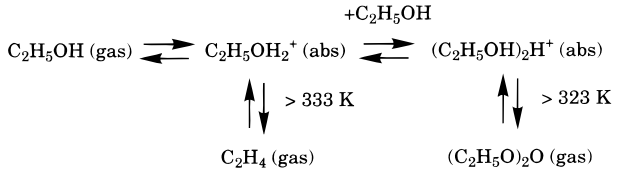

The unusual pressure dependencies of the rate, selectivity, and the amount of absorbed ethanol are interpreted by the following mechanism. Plausible reaction intermediates in this mechanism such as protonated ethanol dimer, $(C_2H_5OH)_2H^+$, monomer, $C_2H_5OH_2^+$, and ethoxy group coordinated with polyanion were directly detected by solid-state NMR, as described before.[59]

Recently, Shikata et al. have found that MTBE synthesis from isobutylene and methanol was efficiently catalyzed by a Dawson HPA, $H_6P_2W_{18}O_{62}$, at low temperatures where the equilibrium favors the ether synthesis.[52] The catalytic activity changed in the order of $H_6P_2W_{18}O_{62} \gg H_3PW_{12}O_{40} > H_4SiW_{12}O_{40} \approx H_4GeW_{12}O_{40} > H_5BW_{12}O_{40} > H_6CoW_{12}O_{40}$, whereby the selectivity to MTBE was higher than 95%. The activity of $H_6P_2W_{18}O_{62}$ was comparable with an ion-exchange resin and much better than SO_4^{2-}/ZrO_2, SiO_2-Al_2O_3, and H-ZSM-5.

The MTBE synthesis proceeds in the pseudoliquid phase and the absorption/desorption property seemed to control the reaction rate.[52] Isobutylene probably absorbs, being assisted by polar methanol molecules. In the pseudoliquid phase of the Dawson HPAs, the rate of methanol absorption is rapid and the amount of methanol absorbed is moderate to form active pseudoliquid phase as was observed for dehydration,[59,144,145] probably due to its amorphous and flexible secondary structure. The Keggin HPAs tended to form a stable structure absorbing a much greater amount of reactant and becomes less active. The marked difference between Dawson and Keggin HPAs is presumably brought about by the shape of the polyanion itself (ellipsoid for Dawson vs spherical for Keggin).[52] Supporting $H_6P_2W_{18}O_{62}$ on SiO_2 greatly increased the yield of MTBE, but decreased the merit due to the pseudoliquid behavior of Dawson HPAs. Hence, in the case of MTBE synthesis, the rates of reaction and diffusion of reactant may be comparable.

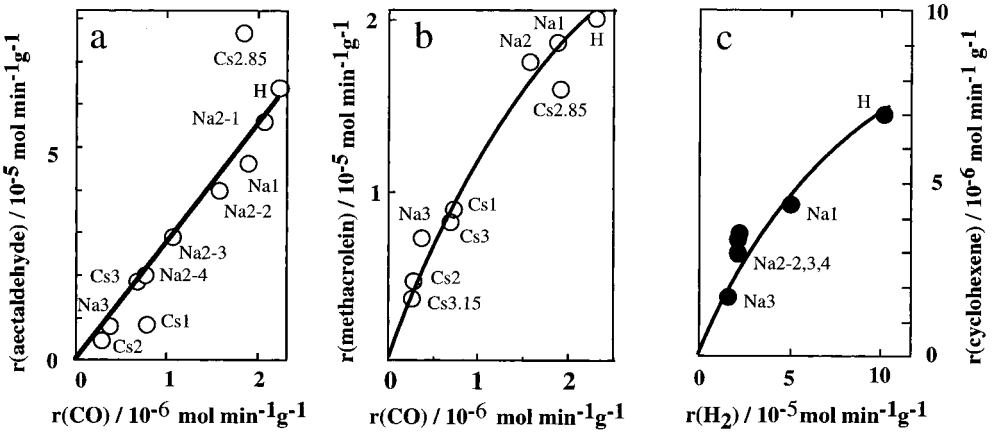

Figure 9. Correlations between catalytic activity and oxidizing ability for oxidation of (a) acetaldehyde and (b) methacrolein (surface reactions) and (c) oxidative dehydrogenation of cyclohexene (bulk-type (II) reaction). *r*(acetaldehyde), *r*(methacrolein), and *r*(cyclohexene) are the rates of catalytic oxidation of acetaldehyde, methacrolein, and oxidative dehydrogenation of cyclohexene, respectively. *r*(CO) is the rate of reduction of catalysts by CO; $r(H_2)$, rate of reduction of catalysts by H_2. M_x denotes $M_xH_{3-x}PMo_{12}O_{40}$. Na2-1, -2, -3, and -4 are $Na_2HPMo_{12}O_{40}$ of different lots, of which surface areas are 2.8, 2.2, 1.7, and 1.2 $m^2\ g^{-1}$, respectively.

Table 3. Comparison of Rates of Reactions and Degree of Reduction at Stationary State of $H_3PMo_{12}O_{40}$ at 623 K[a]

reactions	H_2	CO
catalytic oxidation	130	2.4
reduction of catalyst	110	3.1
reoxidation of catalyst by O_2	110	2.6
degree of reduction of catalyst	0.30	0.038

[a] Rates are in the unit of 10^{-3} electron anion^{-1} min^{-1} and degree of reduction in electron anion^{-1}.

3. Bulk-Type (II) Catalysis

Certain oxidation reactions like oxidative dehydrogenation and oxidation of hydrogen at high temperatures exhibit bulk-type (II) catalysis.[105] In this type of catalytic oxidation, although the principal reaction may proceed on the surface, the whole solid bulk takes part in redox catalysis owing to the rapid migration of redox carriers such as protons and electrons. The rate is proportional to the volume of catalyst in the ideal bulk-type (II) catalysis.

Figure 9a−c shows the correlations between the oxidizing ability of catalysts and the catalytic activity for oxidation.[147−150] Monotonous correlations were observed between the rates of catalytic oxidation of acetaldehyde and methacrolein (surface-type reaction) and the rate of reduction of catalysts by CO (surface oxidizing ability).[148,149] A similar good relationship for oxidative dehydrogenation of cyclohexene (bulk-type (II) reaction) and the rate of reduction of catalysts by hydrogen (bulk oxidizing ability) was found (Figure 9c).[150]

A redox (or Mars−van Krevelen) mechanism has been demonstrated for the catalytic oxidation of hydrogen (bulk-type (II)) and CO (surface-type) over alkali salts of $H_3PMo_{12}O_{40}$; the rates of catalytic oxidation, the rates of reduction and reoxidation of catalysts coincided with each other at the stationary oxidation state of catalyst as summarized in Table 3.[105,110] Due to the thermal instability, no such correlations have been established for $H_{3+x}PMo_{12-x}V_xO_{40}$ ($x \geq 1$).

B. Heterogeneous Acid-Catalyzed Reactions

1. General Characteristics

Acidity, basicity, and pseudoliquid behavior are the principal factors governing the acid catalysis of solid HPAs. The acidic properties are mainly controlled by (i) the structure and composition of the heteropolyanion itself, (ii) the countercations, and (iii) the dispersion on supports. The acid strength can be controlled mainly by i, and the number of acid sites is greatly influenced by ii and iii. The secondary and tertiary structures are also affected by the three factors. In addition to the acidic properties, the absorption properties for polar molecules are critical in determining the catalytic function in the case of "pseudoliquid" catalysis. Besides, soft basicity of the heteropolyanion itself sometimes plays an important role for high catalytic activity. Although the relationship between basicity and solubility of Ag_nX and AgI is not evident, the soft basicity of polyanion as estimated by the equilibrium constant in aqueous solution of the reaction, $Ag_nX + nNaI \rightleftharpoons nAgI + Na_nX$ (X = polyanion), was in the order of $SiW_{12}O_{40}^{4-} > GeW_{12}O_{40}^{4-} > PW_{12}O_{40}^{3-} > PMo_{12}O_{40}^{3-} > SiMo_{12}O_{40}^{4-} > SO_4^{2-}$.[151,152] Although the role has not sufficiently been clarified, it seems that successful industrial applications in the liquid phase take advantage of this soft basicity.

The acidity of hydrogen forms in the solid state reflects in general the acidity in solution; the acid strength decreases when W is replaced by Mo and when the central P atom is replaced by Si for Keggin HPAs, which are stronger acids than Dawson HPAs.[77] The acid strength for Keggin 12-tungstates in acetonitrile solution increased with an increase in the charge of heteropolyanion.[153] The rates of heterogeneous alkylation of 1,3,5-trimethylbenzene catalyzed by the hydrogen forms of several 12-tungstates are correlated well with the negative charge of polyanion.[153,154] This correlation indicates that the acid strength of the hydrogen form of 12-tungstates in the solid state reflects that in solution and decreases with increasing negative charge of the polyanion. On the

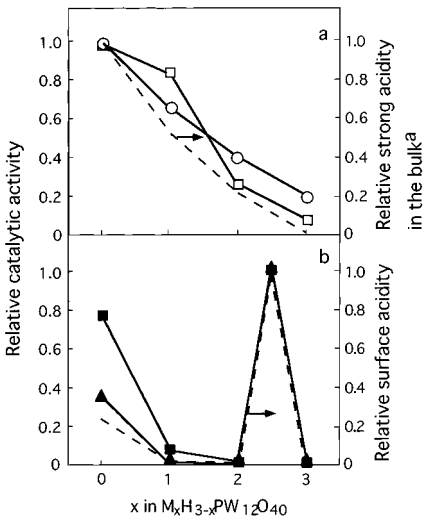

Figure 10. Catalytic activities of acidic Na or Cs salts of $H_3PW_{12}O_{40}$ as a function of Na or Cs content: (a) M = Na; (○) dehydration of 2-propanol, (□) conversion of methanol; and (b) M = Cs; (▲) alkylation of 1,3,5-trimethylbenzene with cyclohexene, (■) conversion of dimethyl ether. Broken lines in parts a and b indicate bulk and surface acidity, respectively. [a] Number of pyridine molecules per anion which remained after the evacuation of 573 K.

other hand, it was reported for HPAs of Mo that the acid strength in solution is not correlated with that in the solid.[50]

A remarkable effect of the countercation is shown in Figure 10a,b, where the reaction rates of several reactions are plotted against the extent of neutralization by Na or Cs, that is, x in $M_xH_{3-x}PW_{12}O_{40}$ (M = Na or Cs).[95,155] In the case of Na salts, the rates decrease more or less monotonically as the Na content increases. This change is in parallel with the change in the bulk acidity shown by the broken line in Figure 10a. Peculiar changes in activity are observed for the Cs salts (Figure 10b); maxima at x = 0 and 2.5, have been interpreted by the change in the surface acidity (= surface area multiplied by proton density on the surface) shown by the broken line in Figure 10b.[95,155]

Figure 11 shows the linear correlation between the catalytic activities and the surface acidity (data are from symbols ▲ in Figure 10b). The catalytic activity increased linearly with the surface acidity. The results indicate that the acid strengths of acidic Cs salts are similar to that of the acid form, as is consistent with the results of ammonia-TPD. Thus, the high catalytic activity of $Cs_{2.5}H_{0.5}PW_{12}O_{40}$ is primarily due to the high surface acidity.

It is remarkable that the catalytic activities of $Cs_{2.5}H_{0.5}PW_{12}O_{40}$ for these reactions are much higher than those of SiO_2-Al_2O_3, SO_4^{2-}/ZrO_2, and HY zeolite. Since the acid strength of $Cs_{2.5}H_{0.5}PW_{12}O_{40}$ is estimated to be between zeolite and SO_4^{2-}/ZrO_2 and the acid amount was much less than those of SiO_2-Al_2O_3, SO_4^{2-}/ZrO_2, and HY zeolite, there must be additional effects such as acid−base bifunctional acceleration by the cooperation of proton (acid) and polyanion (base) (see the much greater slope for $Cs_xH_{3-x}PW_{12}O_{40}$ than the other solid acids in Figure 11).[95]

The catalyst deactivation is usually observed during the catalytic reaction, and the deactivation is

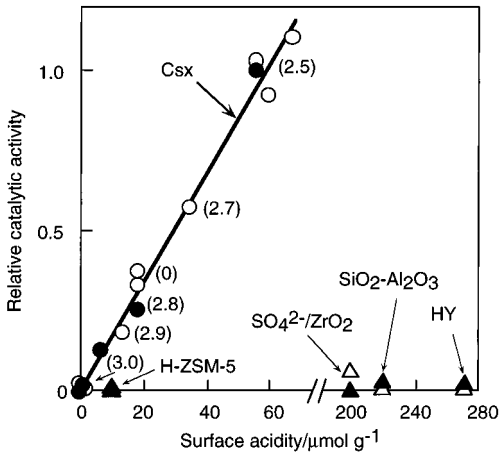

Figure 11. Surface acidity and catalytic activities for alkylation of 1,3,5-trimethylbenzene with cyclohexene (closed symbols) and decomposition of cyclohexyl acetate (open symbols). Numbers in parentheses denote x in Cs_x-$H_{3-x}PW_{12}O_{40}$.

sensitive to the kind of reactant, product, solvent, and reaction temperature. There are several possible causes for the catalyst deactivation, e.g., coke formation, adsorption of products, catalyst reduction, catalyst decomposition, and catalyst dissolution. Deactivation due to reduction was observed, for example, for the dehydration of 2-propanol catalyzed by HPAs containing Mo and V. An oxygen treatment of the deactivated $H_3PMo_{12}O_{40}$ restored the initial catalytic activity,[156] while no such deactivation was observed for HPAs of W. The coke formation or strong adsorption of polymerized products often causes deactivation as in the case of other solid acids.

Therefore, the suppression of the deactivation and the method of regeneration are the important problems in the acid catalysis of HPAs. The selection of a catalyst having uniform and appropriate acid strength is a way to avoid the catalyst deactivation: This may be the reason for the little deactivation observed in the isomerization of butene catalyzed by $H_3PW_{12}O_{40}\cdot 6H_2O$.[156] The deactivation of $Cs_{2.5}H_{0.5}$-$PW_{12}O_{40}$ catalyst due to the coke formation for the isomerization of *n*-pentane was much suppressed by the presence of hydrogen and Pt/Al_2O_3. Hydrogen atom spilt over from Pt probably removes the coke precursor by hydrogenation. What is more interesting is that the deactivation was almost absent in this case in contrast to the large deactivation of SO_4^{2-}/ZrO_2 + Pt/Al_2O_3 as shown in Figure 12.[157] This is presumably brought about by the uniform and moderate acid strength of HPA.[157]

2. Shape-Selective Acid Catalysis

Figure 13 shows the time courses of the adsorption of cyclohexyl acetate (0.60 nm) and isopropyl acetate (0.50 nm) on $Cs_{2.2}H_{0.8}PW_{12}O_{40}$ and $Cs_{2.5}H_{0.5}PW_{12}O_{40}$.[24] Both cyclohexyl acetate and isopropyl acetate were adsorbed on $Cs_{2.5}H_{0.5}PW_{12}O_{40}$. The ratio of the adsorption isopropyl acetate to cyclohexyl acetate was about 1.5, which was close to the ratio of the molecular cross section of the two molecules. On the other hand, the adsorption of cyclohexyl acetate was about 1/10 that of isopropyl acetate on $Cs_{2.2}H_{0.8}PW_{12}O_{40}$ as

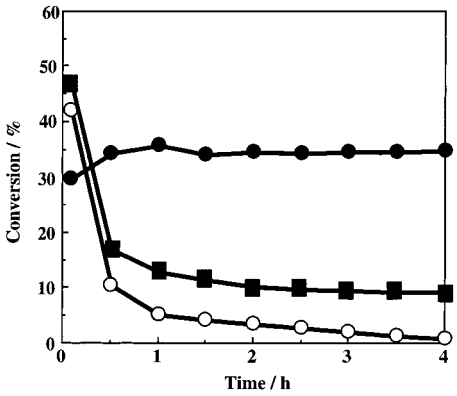

Figure 12. Skeletal isomerization of *n*-pentane at 453 K: (●) $Cs_{2.5}H_{0.5}PW_{12}O_{40}$ mechanically mixed with Pt(1 wt %)/Al_2O_3; (■) SO_4^{2-}/ZrO_2 mechanically mixed with Pt(1 wt %)/Al_2O_3; (○) $Cs_{2.5}H_{0.5}PW_{12}O_{40}$.

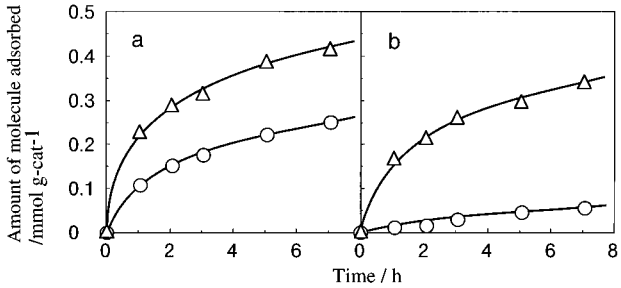

Figure 13. Time courses of the adsorption of isopropyl acetate (△) or cyclohexyl acetate (○) on (a) $Cs_{2.5}H_{0.5}PW_{12}O_{40}$ and (b) $Cs_{2.2}H_{0.8}PW_{12}O_{40}$.

shown in Figure 13b. This result demonstrates that the adsorption of large molecules into the pore of the latter is difficult and that the shape selectivity exists in adsorption.

The shape selective adsorption is well reflected in the catalysis. $Cs_{2.2}H_{0.8}PW_{12}O_{40}$ effectively catalyzed the dehydration of 2-hexanol (molecular size 0.50 nm) and the decomposition of isopropyl acetate (0.50 nm), but was much less active for the reactions of larger molecules such as cyclohexyl acetate (0.60 nm) and 1,3,5-trimethylbenzene (0.75 nm).[24,37] This is in contrast to $Cs_{2.5}H_{0.5}PW_{12}O_{40}$, for which high reaction rates were observed for all of these reactions.

It was reported that $H_3PW_{12}O_{40}$ supported on mesoporous silica molecular sieve, MCM-41, exhibited a higher activity than H_2SO_4 in liquid-phase alkylation of 4-*tert*-butylphenol with isobutene and styrene. In the latter reaction, the catalyst gave a higher yield of 2-(1-phenylethyl)-4-*tert*-butylphenol than more bulky 2,6-bis(1-phenylethyl)-4-*tert*-butylphenol and is claimed to be a size-selective catalyst.[91] Recently, it was found that the impregnation of MCM-41 with an aqueous solution of $H_3PW_{12}O_{40}$ gave two species. One is an intact Keggin structure and the other is $H_6P_2W_{18}O_{62}$ and/or $H_6P_2W_{21}O_{71}$. The latter species was suggested to be about 8 times more active than the former species in the liquid-phase *trans*-de-*tert*-butylation of 2,6-di-*tert*-butyl-4-methylphenol.[158]

The isobutane alkylation with 2-butene catalyzed by $H_3PW_{12}O_{40}$ supported on MCM-41 was compared with those for MCM-22, $H_3PW_{12}O_{40}/SiO_2$, and $H_3PW_{12}O_{40}/Al_2O_3$. The conversion of $H_3PW_{12}O_{40}$/MCM-41 was 87%. The trimethylpentane to dimehylhexane ratio for $H_3PW_{12}O_{40}$/MCM-41 was higher than those for $H_3PW_{12}O_{40}/SiO_2$ and $H_3PW_{12}O_{40}/Al_2O_3$, but less than that for MCM-22.[159]

Table 4. Comparison of Catalytic Activity with Other Solid Acids

solid acid	benzylation of benzene:[a] $PhCH_2Cl$ conversion, %	benzoylation of *p*-xylene:[b] PhCOCl conversion, %
$H_3PW_{12}O_{40}$	41	30
$Cs_{2.5}H_{0.5}PW_{12}O_{40}$	75	57
$Cs_{2.5}H_{0.5}PMo_{12}O_{40}$	93	
$Cs_2H_2SiW_{12}O_{40}$	99	12
$(NH_4)_2HPW_{12}O_{40}$[c]	100	77
HY	36	9
LaY	50	9
Nafion-H	24	48
Zn-montmorillonite[d]	100	35[e]

[a] Benzene/benzyl chloride = 100/5 mmol, catalyst 65 mg, reflux, 2 h. [b] *p*-Xylene/benzoyl chloride = 100/5 mmol, catalyst 35 mg, reflux, 2 h. [c] Calcined at 723 K, catalyst 30 mg. [d] Zn^{2+}-ion exchanged montmorillonite. [e] Catalyst 140 mg.

3. Insoluble Solid Acid Catalysts for Liquid-Phase Reactions

Insoluble solid acid catalysts to replace soluble acids are desirable to make the catalytic processes environmentally benign. For this purpose, the hydrogen cesium, ammonium, and cerium salts and the inclusion of HPAs in silica matrix have been proposed.

$Cs_{2.5}H_{0.5}PW_{12}O_{40}$, as an insoluble acid, catalyzed the alkylation of isobutane with butenes and the catalytic activity was higher than that of $H_3PW_{12}O_{40}$ and SO_4^{2-}/ZrO_2, although the problem of catalyst deactivation remains still unsolved in this case.[160] $Cs_{2.5}H_{0.5}PW_{12}O_{40}$ also catalyzed the alkylation of *p*-xylene and was much more active than SO_4^{2-}/ZrO_2.[161] Izumi et al. found that $(NH_4)_2HPW_{12}O_{40}$ worked as an efficient insoluble acid catalyst for the liquid-phase Friedel−Crafts alkylation (benzylation) of benzene and the acylation of *p*-xylene with benzoic anhydride or benzoyl chloride.[162] It was confirmed that $(NH_4)_2HPW_{12}O_{40}$ did not deteriorate during the benzoylation with benzoyl chloride, but gradually lost its activity due to partial dissolution. In contrast, no deterioration was observed for the benzoylation of *p*-xylene with benzoic anhydride catalyzed by the same HPA. As shown in Table 4, $(NH_4)_2HPW_{12}O_{40}$ was much more active than HY, LaY, and Nafion-H and comparable to or higher than $Cs_{2.5}H_{0.5}PW_{12}O_{40}$ and Zn-montmorillonite.

$Cs_{2.5}H_{0.5}PW_{12}O_{40}$ was remarkably active for the hydrolysis of 2-methylphenyl acetate in excess water, while H-ZSM-5, Nb_2O_5, or SO_4^{2-}/ZrO_2 was almost inactive.[163]

The liquid-phase esterification of 2,6-pyridinedicarboxylic acid with *n*-BuOH is efficiently catalyzed by using an insoluble acidic Ce(III) salt of $H_3PW_{12}O_{40}$, $Ce_{0.87}H_{0.4}PW_{12}O_{40}$.[164] The catalytic activity decreased in the order of $Ce_{0.87}H_{0.4}PW_{12}O_{40} \gg Cs_{2.5}H_{0.5}PW_{12}O_{40} \geq Cs_3PW_{12}O_{40} \geq Cs_2HPW_{12}O_{40} \geq (NH_4)_3PW_{12}O_{40} > K_3PW_{12}O_{40}$. Since the soluble $H_3PW_{12}O_{40}$ was the most active, the possibility of partial dissolution of

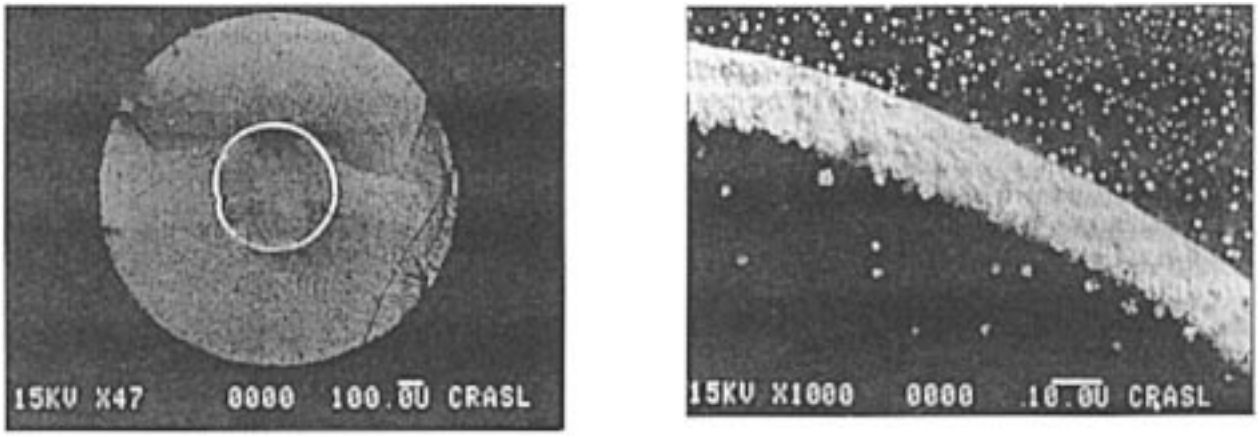

Figure 14. Backscattered electron image of 40% $Cs_{2.5}H_{0.5}PW_{12}O_{40}$ supported in SiO_2 extrude.

the acidic salts needs to be carefully examined for quantitative comparison.

Izumi et al. prepared $H_3PW_{12}O_{40}$ and $Cs_{2.5}H_{0.5}PW_{12}O_{40}$ which were included in a silica matrix by in situ preparation.[165] The catalysts had large surface areas, were insoluble in aqueous media, and efficiently catalyzed the hydrolysis of ethyl acetate. Leakage of $H_3PW_{12}O_{40}$ into solution during the hydrolysis was as low as 0.3%. It is of interest that the catalytic activity of the silica-included $H_3PW_{12}O_{40}$ is higher than $H_3PW_{12}O_{40}$ in aqueous solution. They suggested that $H_3PW_{12}O_{40}$ formed a highly concentrated aqueous solution in the matrix and was therefore more active. The fixation of $H_3PW_{12}O_{40}$ on activated carbon[70−72] and Amberlyst-15[73,74] is also effective for the heterogeneous liquid-phase catalysis as described section II.E.

More recently, $Cs_{2.5}H_{0.5}PW_{12}O_{40}$ supported in spherical particles of SiO_2 gel was reported.[166,167] SiO_2 was preimpregnated by Cs ions to form surface Si−O−Cs groups. Energy dispersive X-ray spectroscopy confirmed uniform Cs distribution at this stage. This then was subjected to impregnation by an aqueous solution of $H_3PW_{12}O_{40}$. Insoluble Cs salts were precipitated in the particles to form a beautiful eggwhite-type distribution in the SiO_2 particle as shown in Figure 14. The backscattered electron image and EDS measurements indicated that Cs and W are present in the white areas. Nearly 80−90% of the $Cs_{2.5}H_{0.5}PW_{12}O_{40}$ is present in a ring about 10 μm thick located more than half way into the $^1/_{16}$ in. diameter extrudates.

C. Heterogeneous Oxidation Reactions

1. General Characteristics

Solid HPAs catalyze various oxygenation and oxidative dehydrogenation reactions. Keggin HPAs containing Mo and V as addenda atoms are usually used for the oxidations. So far the oxidation of methacrolein to methacrylic acid is the only large-scale commercialized process using HPAs. But, ethylene to acetic acid process will start soon. HPAs show a good performance also for oxidative dehydrogenation of isobutyric acid to methacrylic acid but the performance is insufficient for commercialization.

The catalysts reported in patents for heterogeneous oxidation contain several elements other than Mo, V, and P. An excess amount of P was added in patent literature, which was claimed to stabilize the structure. The addition of transition elements like Cu improves redox reversibility. Cs is often added probably to enhance the thermal stability and surface area by forming Cs salts. As for the structure of Cs-containing HPAs, the formation of an epitaxial thin film of the hydrogen form on high-surface area Cs salt was suggested.[26] On the other hand, we reported that a nearly uniform solid solution was formed for $Cs_xH_{3-x}PW_{12}O_{40}$ by the diffusion of Cs and H.[2,23−25] The real catalyst may be in between the two extremes.

To understand the oxidation catalysis of solid HPAs, the contrast between surface- and bulk-type (II) catalysis, and acid−redox bifunctionality of heteropoly catalysts must be properly taken into account, in addition to the correlation between the oxidizing ability of catalysts and their catalytic activity.[1,2,4,105,106,147,168] Interestingly, the two oxidation reactions described above to form methacrylic acid belong to surface- and bulk-type catalysis, respectively.[147]

The fundamental correlations between the redox properties and catalytic activity have successfully been established for the hydrogen form and alkali salts of 12-molybdophosphoric acid as described in the previous section.[1,2,4] However, such correlations have not been obtained for mixed-addenda HPAs due to insufficient thermal stability.[1,2,4,47,48] We attempted to stabilize the mixed coordinated HPAs such as molybdovanadophosphates by forming their cesium salts. Although the possibility of slight decomposition could not be excluded, high yields were obtained for the conversion of isobutyric acid to methacrylic acid as shown in Figure 15.[33] In this case, not only the thermal stability and surface area, but also the acid−base property changes very much with the Cs content, as indicated by the change in the product distribution.

2. Oxidation of Alkanes with Molecular Oxygen

There have been several attempts to obtain oxygenated products from lower alkanes (C_2−C_5) by using heteropoly catalysts. It has been reported that $H_3PMo_{12}O_{40}$ catalyzes the oxidation of lower alkanes, especially propane, isobutane, and pentane, and that

Table 5. Oxidation of Isobutane Catalyzed by $Cs_xH_{3-x}PMo_{12}O_{40}$ and $Cs_{2.5}Ni_{0.08}H_{1.34}PVMo_{11}O_{40}$ at 613 K[a]

catalyst	surface area, $m^2\ g^{-1}$	conv, %	rate, 10^{-5} mol $min^{-1}\ m^{-2}$	selectivity,[b] %					sum of yields of MAA + MAL, %
				MAA	MAL	AcOH	CO	CO_2	
$x = 0$	1.1	7	1.34	4	18	8	44	26	1.5
1	2.1	6	0.60	23	17	10	32	18	2.4
2	5.9	11	0.39	34	10	7	29	21	4.8
2.5	9.5	16	0.36	24	7	7	41	21	5.1
2.85	46.0	17	0.08	5	10	5	44	37	2.4
3[c]	46.0	8	0.04	0	10	6	32	35	0.8
$Cs_{2.5}Ni_{0.08}H_{1.34}PVMo_{11}O_{40}$	40.8	31	0.15	29	4	7	32	28	10.2

[a] Isobutane, 17 vol %; O_2, 33 vol %; N_2, balance; catalyst, 1.0 g; total flow rate, ~30 $cm^3\ min^{-1}$. [b] Calculated on the C_4 (isobutane) basis. [c] The selectivity to acetone was 17%.

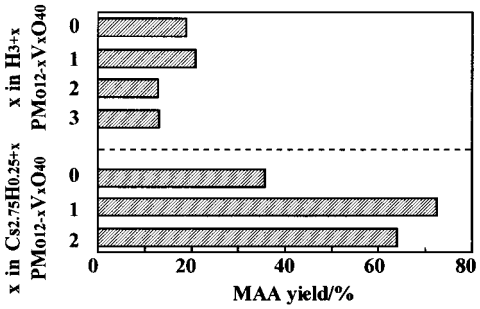

Figure 15. Effect of V and Cs contents on the yield of methacrylic acid (MAA) at 623 K catalyzed by $H_{3+x}PMo_{12-x}V_xO_{40}$ and $Cs_{2.75}H_{0.25+x}PMo_{12-x}V_xO_{40}$.

the substitution of V^{5+} for Mo^{6+} improves the catalytic activity and selectivity.[1,169−176]

By optimizing the constituent elements of heteropolyanions and the countercations, fairly good yields were obtained for the oxidation of isobutane toward methacrylic acid (MAA) and methacrolein (MAL).[177−184] The results on $Cs_xH_{3-x}PMo_{12}O_{40}$ catalysts are shown in Table 5. The highest conversion and yield of MAA were observed around $x = 2.5-2.85$. The catalytic properties of $Cs_{2.5}H_{0.5}PMo_{12}O_{40}$ also changed by the addition of transition metal ions.[177] The addition of Ni, Mn, or Fe increased the yields of MAA and MAL. In the case of Ni, the yields of MAA and MAL reached 6.5 and 1.5%, respectively. In contrast, the addition of Co, Cu, Hg, Pt, and Pd decreased the yields.

Keggin V-substituted heteropolymolybdates, $Cs_{2.5}Ni_{0.08}H_{1.34}PVMo_{11}O_{40}$, catalyzed more selectively the oxidation of isobutane into methacrolein and methacrylic acid. At 613 K the yield of methacrylic acid reached 9.0%. This yield was greater than the highest value of 6.2% reported at likely steady state in the patent literature.[178] $Cs_{2.5}M^{n+}{}_{0.08}H_{1.5-0.08n}PVMo_{11}O_{40}$ (M = Ni^{2+}, Fe^{3+}) also catalyzed the oxidation of propane and ethane.[182−184]

It is interesting that the reduced HPAs showed higher selectivities to methacrylic acid for the oxidation of isobutane.[58,177,180,185] Ueda et al. applied prereduced 12-molybdophosphoric acid to the oxidation of propane and obtained 50% selectivity to acrylic acid and acrolein at 12% conversion.[58]

The conversion vs selectivity relationships of oxidation of isobutane catalyzed by $Cs_{2.5}Ni_{0.08}H_{0.34}PMo_{12}O_{40}$ showed that the reaction proceeds according to Scheme 2. For example, the selectivities to MAL and COx extrapolated to 0% conversion were ~75% and 25%, respectively, indicating that there are two parallel paths in the first step, that is, the selective oxidation of isobutane into MAL and the complete oxidation to COx. The selectivity to MAL decreased with an increase in the selectivity to MAA, showing the oxidation of MAL to MAA.[181]

Scheme 2. Reaction Mechanism of Oxidation of Isobutane

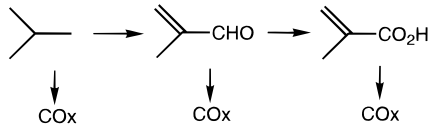

It was suggested from the comparison of the conversion vs selectivity data for $Cs_{2.5}Ni_{0.08}H_{1.34}PVMo_{11}O_{40}$ that the complete oxidation reactions of MAL and MAA are suppressed and the selective oxidation of MAL into MAA is accelerated by the V substitution.[181] The effect of V was recently discussed also for $H_4PVMo_{11}O_{40}$. In this case, it was indicated that V expelled from the polyanion controls the redox property and suppresses the overoxidations of MAL and MAA.[186] The creation of inter-Keggin V−O−V bonds is suggested.[172]

Oxidative dehydrogenation is advantageous in comparison with simple dehydrogenation with respect to equilibrium, since it can achieve much higher conversion of alkanes at low temperatures and high pressures. Cavani et al. reported that Dawson monoiron-substituted heteropolytungstates and Keggin heteropolymolybdates are active for the oxidative dehydrogenation of isobutane[53,187,188] and ethane,[189,190] respectively.

V. Bifunctional Catalysis

A. Acid–Redox Catalysts

The acidity and oxidizing ability work cooperatively in the oxidation of methacrolein:[13]

$$\mathrm{RCHO} \underset{\text{(acid)}}{\rightleftharpoons} \mathrm{RCH(OM)_2} \xrightarrow[\text{(redox)}]{} \mathrm{RCOOM} \rightarrow \mathrm{RCOOH} \quad (4)$$

(M = H or Mo)

The redox mechanism assisted by acidity (eq 4) was confirmed by the several experimental facts.[1] For example, a fair correlation between the rate of catalytic oxidation and the oxidizing ability of catalyst was observed,[13,149] showing that the rate-limiting step is the oxidative dehydrogenation of the inter-

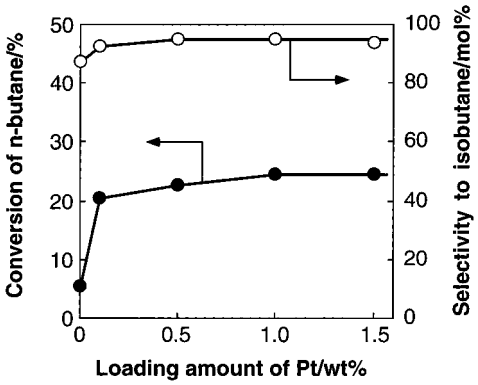

Figure 16. Effect of loading amount of Pt on *n*-butane isomerization over Pt-$Cs_{2.5}H_{0.5}PW_{12}O_{40}$: (●) conversion of *n*-butane, and (○) selectivity to isobutane. Conditions: feed gas, *n*-butane:H_2:N_2 = 0.05:0.50:0.45; catalyst, 1 g; W/F = 40 g h (*n*-butane mol)$^{-1}$. Catalysts were pretreated with O_2 at 573 K.

mediate (second step). Rapid and direct exchanges of isotopic oxygen exist between methacrolein, water, and catalyst, supporting the presence of preequilibrium for the first step.[13,149] The first step in eq 4 is catalyzed by Brønsted acid, but is not rate limiting.

Competitive function of acidity and oxidizing ability was indicated by the changes in the selectivity for the dehydrogenation of isobutyric acid[191] and methanol.[192]

B. Metal–HPA Composite Catalysts

The skeletal isomerization of C_4, C_5, and C_6 alkanes are efficiently catalyzed by Pd salt of $H_3PW_{12}O_{40}$[193−195] and Pd- or Pt-$Cs_{2.5}H_{0.5}PW_{12}O_{40}$ catalysts.[41,54,196−198] In the case of $Pd_{1.5}PW_{12}O_{40}$ as described before, protons are generated by the reaction of Pd^{2+} with hydrogen. The presence of hydrogen is necessary to maintain the high activity at the stationary state.

As for Pt with $Cs_{2.5}H_{0.5}PW_{12}O_{40}$, the effect of loading amount of Pt on the skeletal isomerization of *n*-butane to isobutane is shown in Figure 16.[41,54,196−198] The reaction at the steady state was accelerated by a factor of about 4 by the addition of 0.1 wt % Pt, and the rate and selectivity became constant above 0.1 wt % Pt. Isobutane was formed for Pt- and Pd-$Cs_{2.5}H_{0.5}PW_{12}O_{40}$ catalysts with high selectivities (94−96%) and high rates. Hydrogen suppresses the catalyst deactivation by lowering the partial pressure of butenes and hydrogenating coke or precursor of the coke. Pt-$Cs_{2.5}H_{0.5}PW_{12}O_{40}$ also showed higher activity and selectivity than Pt-SO_4^{2-}/ZrO_2 and Pt-Al_2O_3 for the skeletal isomerization of *n*-pentane and *n*-hexane.[157]

It was demonstrated that the high selectivity to isobutane for Pt-$Cs_{2.5}H_{0.5}PW_{12}O_{40}$ is brought about by the unique roles of protons which suppress dramatically the hydrogenolysis and enhance the isomerization. For example, when a small amount of $H_3PW_{12}O_{40}$ was impregnated onto Pt-$Cs_3PW_{12}O_{40}$, the isomerization of *n*-butane proceeded rapidly and very selectively, and the hydrogenolysis on Pt-$Cs_3PW_{12}O_{40}$ nearly completely stopped. This effect was not pronounced for the isomerization of *n*-pentane and *n*-hexane, since hydrogenolysis little took place on Pt-$Cs_3PW_{12}O_{40}$ due to lower reaction temperatures. Scheme 3 illustrates this phenomenon.[197,198] In the absence of proton, the hydrogenolysis proceeds on Pt, while in the presence of proton only the selective isomerization proceeds.

Scheme 3. A Proposed Reaction Scheme for Isomerization of *n*-Butane

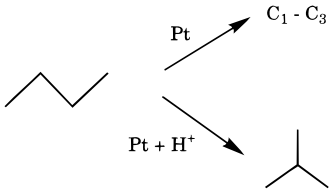

Heterogeneous gas−solid Wacker-type oxidation of butene to methyl ethyl ketone catalyzed by $H_{3+n}PV_nMo_{12-n}O_{40}$ in combination with Cu^{2+}, Ni^{2+}, Pd^{2+}, and Cs^+ salts has been reported, but there was significant catalyst deactivation.[199] Reoxidation of the reduced HPAs was a slow step, which was somehow accelerated by the presence of vanadium, Cu^{2+}, or Ni^{2+}. The combination of Pd and HPA is applied to the commercial oxidation of ethylene to acetic acid.

Pd-$Cs_{2.5}H_{0.34}PVMo_{11}O_{40}$-catalyzed selective oxidation of methane into formic acid with molecular oxygen in the presence of hydrogen at and above 423 K.[200] No selective oxidation proceeded without Pd or when carbon monoxide was used instead of hydrogen. The addition of 1.9 vol % hydrogen peroxide in place of hydrogen and oxygen showed a similar conversion and selectivity to oxygenates. This suggests that the active oxygen species comes from hydrogen peroxide formed by the hydrogen−oxygen reaction catalyzed by Pd. Formic acid was also formed by the liquid-phase oxidation of methane with hydrogen peroxide catalyzed by $H_4PVMo_{11}O_{40}$.[201]

VI. Future Opportunities

Future targets of research are all related to the advantageous properties of HPAs. Progresses are anticipated in the research areas of (1) design of solid acids stronger than superacid of $H_3PW_{12}O_{40}$ and acids having moderate but uniform acid strengths, (2) design of inorganic synzymes (e.g., Fe,Mn-multisubstituted heteropolyanions) and the application to catalysis, (3) bifunctional acid−base or acid−redox catalysis, (4) utilization of the unique properties such as pseudoliquid and controlled pores of the assembly of HPAs for stereoselective and shape-selective reactions, and (5) synthesis and utilization of HPAs of novel structures and compositions.

VII. References

(1) Okuhara, T.; Mizuno, N.; Misono, M. *Adv. Catal.* **1996**, *41*, 113.
(2) Misono, M. In *Proc. 10th Int. Congr. Catal., Budapest, 1992*; Elsevier: Amsterdam, 1993; p 69.
(3) Misono, M. In *Future Opportunities in Catalytic and Engineering Technology*; Misono, M., Moro-oka, Y., Kimura, S., Eds.; Elsevier: Amsterdam, 1990; p 13.
(4) Misono, M. In *Proc. Climax 4th Intern. Conf. Chem. Uses Molybdenum*; Barry, H. F., Mitchell, P. C. H., Eds.; 1982; p 289.
(5) Misono, M. *Catal. Rev.-Sci. Eng.* **1987**, *29*, 269; **1988**, *30*, 339.

(6) Ono, Y. In *Perspectives in Catalysis*; Thomas, J. M., Zamaraev, K. I., Eds.; Blackwell: London, 1992; p 341.
(7) Kozhevnikov, I. V.; Matveev, K. I. *Appl. Catal.* **1983**, *5*, 135.
(8) Izumi, Y.; Urabe, K.; Onaka, A. In *Zeolite, Clay, and Heteropoly-acids in Organic Reactions*; Kodansha: Tokyo; VCH: Weinheim, 1992.
(9) Kozhevnikov, I. V. *Catal. Rev.-Sci. Eng.* **1995**, *37*, 311.
(10) Izumi, Y. *Catal. Today* **1997**, *33*, 371.
(11) Corma, A. *Chem. Rev.* **1995**, *95*, 559.
(12) Misono, M.; Nojiri, N. *Appl. Catal.* **1990**, *64*, 1. Nojiri, N.; Misono, M. *Appl. Catal.* **1993**, *93*, 103.
(13) Misono, M.; Sakata, K.; Yoneda, Y.; Lee, W. Y. In *Proc. 7th Int. Congr. Catal., Tokyo, 1980*; Kodansha: Tokyo; Elsevier: Amsterdam, 1981; p 1047.
(14) Pope, M. T.; Müler, A. *Angew. Chem., Int. Ed. Engl.* **1991**, *30*, 34. In *Polyoxometalates: From Platonic Solids to Anti-Retroviral Activity*; Pope, M. T., Müler, A., Eds.; Kluwer: Dordorecht, 1994.
(15) (a) Jeannin, Y.; Herve, G.; Proust, A. *Inorg. Chim. Acta* **1992**, *189*, 319. (b) Weakley, T. J. R. *Struct. Bond.* **1974**, *18*, 131.
(16) Niiyama, H.; Saito, Y.; Echigoya, E. In *Proc. 7th Int. Congr. Catal., 1980*; Kodansha: Tokyo; Elsevier: Amsterdam, 1981; p 1416.
(17) Kazanskii, L. P.; Potapova, I. V.; Spitsyn, A. V. I. *Dokl. Akad. Nauk SSSR* **1977**, *235*, 387.
(18) Misono, M.; Mizuno, N.; Katamura, K.; Kasai, A.; Konishi, Y.; Sakata, K.; Okuhara, T.; Yoneda, Y. *Bull. Chem. Soc. Jpn.* **1982**, *55*, 400.
(19) Mizuno, N.; Katamura, K.; Misono, M.; Yoneda, Y. *J. Catal.* **1983**, *83*, 384.
(20) Mizuno, N. Master Thesis, The University of Tokyo, 1982.
(21) Lee, K. Y.; Mizuno, N.; Okuhara, T.; Misono, M. *Bull. Chem. Soc. Jpn.* **1989**, *62*, 1731.
(22) Kozhevnikov, I. V.; Sinnema, A.; Jansen, R. J. J.; van Bekkum, H. *Catal. Lett.* **1994**, *27*, 187. Kozhevnikov, I. V.; Sinnema, A.; van Bekkum, H. *Catal. Lett.* **1995**, *34*, 213. Kozhevnikov, I. V.; Sinnema, A.; van Bekkum, H.; Fournier, M. *Catal. Lett.* **1996**, *41*, 153.
(23) Okuhara, T.; Nishimura, T.; Watanabe, H.; Na, K.; Misono, M. In *Acid-Base Catalysis II*; Kodansha: Tokyo; Elsevier: Amsterdam, 1994; p 419.
(24) Okuhara, T.; Nishimura, T.; Misono, M. In *Proc. 11th Intern. Congr. Catal.*; Baltimore, 1996; p 581.
(25) Okuhara, T.; Nishimura, T.; Watanabe, H.; Misono, M. *J. Mol. Catal.* **1992**, *74*, 247.
(26) Essayem, N.; Coudurier, G.; Fournier, M.; Vedrine, J. C. *Catal. Lett.* **1995**, *34*, 223.
(27) Brown, G. M.; Noe-Spirlet, M. R.; Busing, W. R.; Levy, H. A. *Acta Crystallogr., Ser. B* **1977**, *33*, 1038.
(28) Shikata, S.; Okuhara, T.; Misono, M. *Shokubai (Catalysts & Catalysis)* **1997**, *39*, 174.
(29) *Crystal Structure of Inorganic Compounds*, LB Neue Series, III/ 7f, Pies/Weiss; Springer: Berlin, p 406.
(30) (a) Hashimoto, M.; Misono, M. *Acta Crystallogr., Ser. C* **1994**, *50*, 231. (b) Oniani, E. S.; Sergienko, V. S.; Chuaev, V. F.; Mistryukov, A. E. *Russ. J. Inorg. Chem.* **1991**, *36*, 1157.
(31) Izumi, Y.; Ono, M.; Ogawa, M.; Urabe, K. *Chem. Lett.* **1993**, 825. Izumi, Y.; Ogawa, M.; Nohara, W.; Urabe, K. *Chem. Lett.* **1992**, 1987.
(32) Nishimura, T. Ph.D. Thesis, The University of Tokyo, 1995.
(33) Lee, K. Y.; Oishi, S.; Igarashi, H.; Misono, M. *Catal. Today* **1997**, *33*, 183.
(34) Mizuno, N.; Misono, M. *Chem. Lett.* **1987**, 967.
(35) Gregg, S. J.; Stock, R. *Trans. Faraday Soc.* **1957**, *53*, 1355. Gregg, S. J.; Tayyab, M. M. *J. Chem. Soc., Faraday Trans. 1* **1978**, *74*, 348.
(36) Taylor, D. B.; McMonagle, J. B.; Moffat, J. B. *J. Colloid Interface Sci.* **1985**, *108*, 2789. MacMonagle, J. B.; Moffat, J. B. *J. Colloid Interface Sci.* **1984**, *101*, 479. Moffat, J. B. *J. Mol. Catal.* **1989**, *52*, 169. Moffat, J. B.; MacMonagle, J. B.; Taylor, D. *Solid State Ionics* **1988**, *26*, 101.
(37) Okuhara, T.; Nishimura, T.; Misono, M. *Chem. Lett.* **1995**, 155.
(38) Inumaru, K.; Nakajima, H.; Ito, T.; Misono, M. *Chem Lett.* **1996**, 559; *J. Phys. Chem.*, in press.
(39) Okuhara, T.; Nishimura, T.; Misono, M. *Chem. Lett.* **1995**, 155.
(40) Yamada, T. ; Johkan, K.; Seki, K.; Nakati, T.; Okuhara, T. *Shokubai (Catalysts & Catalysis)* **1997**, *39*, 194.
(41) Na, K.; Iizaki, T.; Okuhara, T.; Misono, M. *J. Mol. Catal.* **1997**, *115*, 449.
(42) Ito, T.; Song, I.-K.; Inumaru, K.; Misono, M. *Chem. Lett.* **1997**, 727.
(43) Tsigdinos, G. A. *Top. Curr. Chem.* **1978**, *76*, 1.
(44) Chuvaev, V. F.; Popov, K. I.; Spitsyn, V. I. *Dokl. Akad. Nauk SSSR* **1980**, *255*, 892.
(45) Fournier, M.; F-Jantou, C.; Rabia, C.; Hervé, G.; Launay, S. *J. Mater. Chem.* **1992**, *2*, 971.
(46) Bondareva, V. M.; Sandrushkevich, T. V.; Maksimovskaya, R. I.; Plyasova, L. M.; Ziborov, A. V.; Litvak, G. S.; Detusheva, L. G. *Kinet. Catal.* **1994**, *35*, 114.
(47) Cadot, E.; Marchal-Roch, C.; Fournier, M.; Tézé, A.; Hervé, G. *Polyoxometalates: From Platonic Solids to Anti-Retroviral Activity*; Pope, M. T., Müler, A., Eds.; Kluwer: Dordorecht, 1994; p 315.
(48) Bayer, R.; Marchal, C.; Liu, F. X.; Tézé, A.; Hervé, G. *J. Mol. Catal. A: Chem.* **1996**, *110*, 65. Marchal-Roch, C.; Bayer, R.; Moisan, J. F.; Tézé, A.; Hervé, G. *Top. Catal.* **1996**, *3*, 407. Bayer, R.; Marchal-Roch, C.; Liu, F. X.; Tézé, A; Hervé, G. *J. Mol. Catal.* **1996**, *114*, 277.
(49) Konishi, Y.; Sakata, K.; Misono, M. *J. Catal.* **1982**, *77*, 169.
(50) Rocchiccioli-Deltcheff, C.; Aouissi, A.; Bettahar, M. M.; Launay, S.; Fournier, M. *J. Catal.* **1996**, *164*, 16.
(51) Eguchi, K.; Yamazoe, N.; Seiyama, T. *Nippon Kagaku Kaishi* **1981**, 336.
(52) Shikata, S.; Nakata, S.; Okuhara, T.; Misono, M. *J. Catal.* **1997**, *166*, 263. Shikata, S.; Okuhara, T.; Misono, M. *J. Mol. Catal.* **1995**, *100*, 49. Shikata, S.; Okuhara, T.; Misono, M. *Shokubai (Catalysts & Catalysis)* **1997**, *39*, 174.
(53) Cavani, F.; Comuzzi, C.; Dolcetti, G.; Finke, R. G.; Lucchi, A.; Trifiro, F.; Trovarelli, A. *A.C.S. Symp. Ser.* **1996**, *638*, 140.
(54) Na, K.; Nakata, S.; Okuhara, T.; Misono, M. *J. Chem. Soc., Faraday Trans.* **1995**, *91*, 367.
(55) Okuhara, T.; Tatematsu, S.; Lee, K. Y.; Misono, M. *Bull. Chem. Soc. Jpn.* **1989**, *62*, 717.
(56) Akaratiwa, L. S.; Niiyama, H. *J. Chem. Eng. Jpn.* **1990**, *23*, 143. Utada, T.; Sugiura, N.; Nakamura, R.; Niiyama, H. *J. Chem. Eng. Jpn.* **1991**, *24*, 417.
(57) Ueshima, M.; Tsuneki, H.; Shimizu, N. *Hyomen* **1986**, *24*, 582.
(58) Ueda, W.; Suzuki, Y.; Lee, W.; Imaoka, S. *Stud. Surf. Sci. Catal.* **1996**, *101*, 1065. Ueda, W.; Suzuki, Y. *Chem. Lett.* **1995**, 541.
(59) Lee, K. Y.; Arai, T.; Nakata, S.; Asaoka, S.; Okuhara, T.; Misono, M. *J. Am. Chem. Soc.* **1992**, *114*, 2836.
(60) Lee, K. Y.; Kanda, Y.; Mizuno, N.; Okuhara, T.; Misono, M.; Nakata, S.; Asaoka, S. *Chem. Lett.* **1988**, 1175.
(61) Hirano, Y.; Inumaru, K. ; Okuhara, T.; Misono, M. *Chem Lett.* **1996**, 1111.
(62) Kanda, K.; Lee, K. Y.; Nakata, S.; Asaoka, S.; Misono, M. *Chem. Lett.* **1988**, 139.
(63) (a) Olah, G. A.; Namanworth, E. *J. Am. Chem. Soc.* **1967**, *89*, 3576. (b) Birchall, T.; Gillespie, R. J. *Can. J. Chem.* **1965**, *43*, 1045.
(64) Yang, R. T.; Chen, N. *Ind. Eng. Chem. Res.* **1994**, *33*, 825.
(65) Bélanger, R.; Moffat, J. B. *J. Catal.* **1995**, *152*, 179.
(66) Cheng, W.-C.; Luthra, N. P. *J. Catal.* **1988**, *109*, 163.
(67) Nowinska, K.; Fiedorow, R.; Adamiec, J. *J. Chem. Soc., Faraday Trans.* **1991**, *87*, 749.
(68) Rao, K. M.; Gobetto, R.; Lannibello, A.; Zecchina, A. *J. Catal.* **1989**, *119*, 512.
(69) van Veer, J. A. R.; Hendriks, P. A. J. M.; Andrea, R. R.; Romers, E. J. M.; Wilson, A. E. *J. Phys. Chem.* **1990**, *94*, 1831.
(70) Izumi, Y.; Urabe, K. *Chem. Lett.* **1981**, 663.
(71) Jansen, R. J. J.; van Veldhuizen, H. M.; Schwegler, M. A.; van Bekkum, H. *Rec. Trav. Chim. Pays-Bas.* **1994**, *113*, 115.
(72) Schwegler, M. A.; van Bekkum, H.; de Munok, N. A. *Appl. Catal.* **1991**, *74*, 191; **1992**, *80*, 92.
(73) Baba, T.; Ono, Y.; Ishimoto, T.; Morikawa, S.; Tanooka, S. *Bull. Chem. Soc. Jpn.* **1985**, *58*, 2155.
(74) Baba, T.; Ono, Y. *Appl. Catal.* **1986**, *22*, 321.
(75) Lee, J. K.; Song, I. K.; Lee, W. Y.; Kim, J.-J. *J. Mol. Catal. A* **1996**, *104*, 311.
(76) Song, I. K.; Shin, S. K.; Lee, W. Y. *J. Catal.* **1993**, *144*, 348.
(77) Kapustin, G. I.; Brueva, T. R.; Klyachko, A. L.; Timofeeva, M. N.; Kulikov, S. M.; Kozhevnikov, I. V. *Kinet. Katal.* **1990**, *31*, 1017.
(78) Mastihkin, V. M.; Kulikov, S. M.; Nosov, A. V.; Kozhevnikov, I. K.; Mudrakovsky, I. L.; Timofeeva, M. V. *J. Mol. Catal.* **1990**, *60*, 65.
(79) Lefebvre, F. *J. Chem. Soc., Chem. Commun.* **1992**, 756.
(80) Thouvenot, R.; Rocchiccioli-Delcheff, C.; Fournier, M. *J. Chem. Soc., Chem. Commun.* **1991**, 1252.
(81) Thouvenot, R.; Fournier. M.; Rocchiccioli-Delcheff, C. *J. Chem. Soc., Faraday Trans.* **1991**, *87*, 2829.
(82) Rocchicioli-Deltcheff, C.; Amirouche, M.; Fournier, M. *J. Catal.* **1992**, *138*, 445.
(83) Brückman, K.; Che, M.; Haber, J.; Tatibouet, J. M. *Catal. Lett.* **1994**, *25*, 225.
(84) Rocchiccioli-Deltcheff, C.; Amirouche, M.; Herve, G.; Fournier, M.; Che, M; Tatibouet, I. M. *J. Catal.* **1990**, *126*, 591.
(85) Tatibouet, J. M.; Che, M.; Amirouche, M.; Fournier, M.; Rocchiccioli-Deltcheff, C. *J. Chem. Soc., Chem. Commun.* **1988**, 1260.
(86) Fournier, M.; Thouvenot, R.; Rocchiccioli-Deltcheff, C. *J. Chem. Soc., Faraday Trans.* **1991**, *87*, 349.
(87) Fournier, M.; Aouissi, A.; Rocchiccioli-Deltcheff, C. *J. Chem. Soc., Chem. Commun.* **1994**, 307.
(88) Rocchiccioli-Deltcheff, C.; Aouissi, A.; Launay, S.; Fournier, M. *J. Mol. Catal.* **1996**, *114*, 331.
(89) Kasztelan, S.; Payen, E.; Moffat, J. B. *J. Catal.* **1990**, *125*, 45.

(90) Nowinska, K.; Fiedorow, R.; Adamiec, J. *J. Chem. Soc., Faraday Trans.* **1991**, *87*, 749.
(91) Kozhevnikov, I. V.; Sinnema, A.; Jansen, R. J. J.; van Bekkum, H. *Catal. Lett.* **1995**, *30*, 241. Hu, C.; He, Q.; Zhang, Y.; Liu, Y.; Zhang, Y.; Tang, T.; Zhang, J.; Wang, E. *Chem. Commun.* **1996**, 121.
(92) Furuta, M.; Sakata, K.; Misono, M.; Yoneda, Y. *Chem. Lett.* **1979**, 31.
(93) Otake, M.; Onoda, T. *Shokubai (Catalysts & Catalysis)* **1975**, *7*, 13.
(94) Okuhara, T.; Nishimura, T.; Watanabe, H.; Misono, M. *J. Mol. Catal.* **1992**, *74*, 247.
(95) Misono, M.; Okuhara, T. *Chemtech* **1993**, *23*, 23.
(96) Gillespie, R. J. *Acc. Chem. Res.* **1968**, *1*, 202. Olah, G. A.; Prakash, G. K. S.; Sommer, J. In *Superacids*; John Wiley & Sons: New York, 1985.
(97) Auroux, A.; Vedrine, J. C. *Stud. Surf. Sci. Catal.* **1985**, *20*, 311.
(98) Drago, R. S.; Dias, J. A.; Maier, T. O. *J. Am. Chem. Soc.* **1997**, *119*, 7702.
(99) Baba, T.; Ono, Y. *J. Phys. Chem.* **1983**, *87*, 3406. Baba, T.; Nomura, M.; Ono, T.; Ohno, Y. *J. Phys. Chem.* **1993**, *97*, 12888.
(100) Baba, T.; Nomura, M.; Ono, Y.; Kansaki, Y. *J. Chem. Soc., Faraday Trans.* **1992**, *88*, 71.
(101) Baba, T.; Nomura, M.; Ohno, Y.; Hiroyama, Y.; Ono, Y. In *New Aspects of Spillover Effect in Catalysis*; Inui, T., Ed.; Elsevier: 1993; p 81.
(102) Baba, T.; Ono, Y. *J. Phys. Chem.* **1996**, *100*, 9064.
(103) Baba, T.; Hasada, Y.; Nomura, M.; Ohno, Y.; Ono, Y. *J. Mol. Catal. A* **1996**, *114*, 247.
(104) Katamura, K.; Nakamura, T.; Sakata, K.; Misono, M.; Yoneda, Y. *Chem. Lett.* **1981**, 89.
(105) (a)Komaya, T.; Misono, M. *Chem. Lett.* **1983**, 1177. (b) Misono, M.; Mizuno, N.; Komaya, T. In *Proc. 8th Int. Congr. Catal., 1984*; Verlag Chemie: Weinheim, 1984; Vol. 5, p 487.
(106) Yoshida, S.; Niiyama, H.; Echigoya, E. *J. Phys. Chem.* **1982**, *86*, 3150; *Nippon Kagaku Kaishi* **1981**, 1703. Yoshida, S.; Miyata, Y.; Niiyama, H.; Echigoya, E. *J. Phys. Chem.* **1982**, 1873.
(107) Hodnett, B. K.; Moffat, J. B. *J. Catal.* **1985**, *91*, 93.
(108) Ai, M. *Appl. Catal.* **1982**, *4*, 245.
(109) Kim, H. C.; Moon, S. H.; Lee, W. Y. *Chem. Lett.* **1991**, 447.
(110) Mizuno, N.; Watanabe, T.; Misono, M. *J. Phys. Chem.* **1985**, *89*, 80.
(111) Eguchi, K.; Toyozawa, Y.; Yamazoe, N.; Seiyama, T. *J. Catal.* **1983**, *83*, 32.
(112) Otake, M.; Komiyama, Y.; Otaki, T. *J. Phys. Chem.* **1973**, *77*, 2896.
(113) Akimoto, M.; Shima, K.; Ikeda, H.; Echigoya, E. *J. Catal.* **1984**, *86*, 173.
(114) Aboukaïs, A.; Ghoussoub, D.; B-Crusson, E.; Rigole, M.; Guelton, M. *Appl. Catal. A* **1994**, *111*, 109.
(115) Centi, G.; Nieto, J. L.; Iapalucci, C. *Appl. Catal.* **1989**, *46*, 197.
(116) Ai, M. *Appl. Catal.* **1982**, *4*, 245.
(117) Akimoto, M.; Tsuchida, Y.; Sato, K.; Echigoya, E. *J. Catal.* **1981**, *72*, 83.
(118) Akimoto, M.; Shima, K.; Ikeda, H.; Echigoya, E. *J. Catal.* **1984**, *86*, 173. Akimoto, M.; Ikeda, H.; Okabe, A.; Echigoya, E. *J. Catal.* **1984**, *89*, 196.
(119) Mizuno, N.; Misono, M. *J. Phys. Chem.* **1989**, *93*, 3334.
(120) Sanchez, C.; Livage, J.; Launay, J. P.; Fournier, M.; Jennin, Y. *J. Am. Chem. Soc.* **1982**, *104*, 3194. Prados, R. A.; Pope, M. T. *Inorg. Chem.* **1976**, *15*, 2547.
(121) Tsuneki, H.; Niiyama, H.; Echigoya, E. *Chem. Lett.* **1978**, 645.
(122) Taketa, H.; Katsuki, S.; Eguchi, K.; Seiyama, T.; Yamazoe, N. *J. Phys. Chem.* **1986**, *90*, 2959.
(123) Mizuno, N.; Watanabe, T.; Misono, M. *J. Phys. Chem.* **1990**, *94*, 890.
(124) Tamura, Y. Master Thesis, The University of Tokyo, 1985. Onuma, K. Master Thesis, The University of Tokyo, 1987.
(125) Nakamura, O.; Kodama, T.; Ogino, I.; Miyake, Y. *Chem. Lett.* **1979**, 17.
(126) Misono, M.; Igarashi, H.; Katamura, K.; Okuhara, T.; Mizuno, M. In *New Aspects of Spillover Effect in Catalysis*; 1993; p 105.
(127) Sakata, K. Ph.D. Dissertation, The University of Tokyo, 1981.
(128) Akimoto, M.; Ikeda, H.; Okabe, A.; Echigoya, E. *J. Catal.* **1984**, *89*, 196.
(129) Duncan, D. C.; Hill, C. L. *J. Am. Chem. Soc.* **1997**, *119*, 243.
(130) Neumann, R.; Levin, M. *J. Am. Chem. Soc.* **1992**, *114*, 7278.
(131) Hiskia, A.; Papaconstantinou, E. *Inorg. Chem.* **1992**, *31*, 163.
(132) Gamsjaeger, J.; Murmann, R. K. *Adv. Inorg. Nioinorg. Mech.* **1983**, *2*, 317.
(133) Filowitz, M.; Ho, R. K. C.; Klemperer, W. G.; Shum, W. *Inorg. Chem.* **1979**, *18*, 93.
(134) Spitsyn, V. I.; Aistova, R. I.; Vesil'ev, V. N. *Dokl. Akad. Nauk SSSR* **1955**, *104*, 741.
(135) Fedotov, M. A.; Maksimovskaya, R. I.; Begalieva, D. U.; Ll'yasova, A. K. *Izv. Akad. Nauk SSSR* **1980**, *29*, 1025.
(136) Matsumoto, H.; Lee, K. Y.; Misono, M. *61st National Meeting of The Chemical Society of Japan*; Tokyo, 1991.
(137) Zuemecki, S. B. In *Proc. 9th Int. Congr. Catal.*; 1988; Vol. 4, p 1798.
(138) Serwicka, E. M.; Bruckman, K.; Haber, J.; Paukshtis, E. A.; Yurchenko, E. N. *Appl. Catal.* **1991**, *73*, 153.
(139) Bruckman, K.; Haber, J.; Serwicka, E. M. *Faraday Disc. Chem. Soc.* **1988**, *87*, 173.
(140) Taouk, T.; Ghoussoub, D.; Bennani, A.; Crusson, E.; Rigole, M.; Aboukais, A.; Decressain, R.; Fournier, M.; Guelton, M. *J. Chim. Phys.* **1992**, *89*, 435.
(141) Misono, M.; Konishi, Y.; Furuta, M.; Yoneda, Y. *Chem. Lett.* **1978**, 709.
(142) Nishimura, T.; Okuhara, T.; Misono, M. *Chem. Lett.* **1991**, 1695.
(143) Okuhara, T.; Hashimoto, T.; Misono, M.; Yoneda, Y.; Niiyama, H.; Saito, Y.; Echigoya, E. *Chem. Lett.* **1983**, 573. Okuhara, T.; Arai, T.; Ichiki, T.; Lee, K. Y.; Misono, M. *J. Mol. Catal.* **1989**, *55*, 293.
(144) Takahashi, K.; Okuhara, T.; Misono, M. *Chem. Lett.* **1985**, 841.
(145) Misono, M.; Okuhara, T.; Ichiki, T.; Arai, T.; Kanda, Y. *J. Am. Chem. Soc.* **1987**, *109*, 5535.
(146) Knözinger, H. *Angew. Chem., Int. Ed. Engl.* **1968**, *7*, 791.
(147) Misono, M.; Mizuno, N.; Mori, H.; Lee, K. Y.; Jiao, J.; Okuhara, T. *Stud. Surf. Sci. Catal.* **1991**, *67*, 87.
(148) Mori, H.; Mizuno, N.; Misono, M. *J. Catal.* **1990**, *131*, 133.
(149) Mizuno, N.; Watanabe, T.; Misono, M. *Bull. Chem. Soc. Jpn.* **1991**, *64*, 243.
(150) Mizuno, N.; Watanabe, T.; Mori, H.; Misono, M. *J. Catal.* **1990**, *123*, 157.
(151) Baraza, L.; Pope, M. T. *J. Phys. Chem.* **1975**, *79*, 92.
(152) Izumi, Y.; Matsuo, K.; Urabe, K. *J. Mol. Catal.* **1983**, *18*, 299.
(153) Hu, C.; Hashimoto, M.; Okuhara, T.; Misono, M. *J. Catal.* **1993**, *143*, 437. Okuhara, T.; Hu, C.; Hashimoto, M.; Misono, M. *Bull. Chem. Soc. Jpn.* **1994**, *67*, 1186.
(154) Hu, C.; Nishimura, T.; Okuhara, T.; Misono, M. *Sekiyu Gakkaishi* **1993**, *36*, 386.
(155) Tatematsu, S.; Hibi, H.; Okuhara, T.; Misono, M. *Chem. Lett.* **1984**, 865. Okuhara, T.; Kasai, A.; Hayakawa, N.; Yoneda, Y.; Misono, M. *J. Catal.* **1983**, *83*, 121.
(156) Hayakawa, M.; Okuhara, T.; Misono, M.; Yoneda, Y. *Nippon Kagaku Kaishi* **1982**, 356. Hayakawa, M.; Okuhara, T.; Misono, M.; Yoneda, Y. Unpublished result.
(157) Liu, Y.; Koyano, G.; Na, K.; Misono, M. *Appl. Catal. A.*, in press.
(158) Kozhevnikov, I. V.; Kloetstra, K. R.; Sinnema, A.; Zandgergen, H. W.; van Bekkum, H. *J. Mol. Catal.* **1996**, *114*, 287.
(159) Kresge, C. T.; Marler, D. O.; Rau, G. S.; Rose, B. H. U.S. Patent 5366945, 1994.
(160) Okuhara, T.; Yamashita, M.; Na, K.; Misono, M. *Chem. Lett.* **1994**, 1451. Corma, A.; Martínez. A.; Martínez. C. *J. Catal.* **1996**, *164*, 422.
(161) Soeda, H.; Okuhara, T.; Misono, M. *Chem. Lett.* **1994**, 909.
(162) Izumi, Y.; Ogawa, M.; Urabe, K. *Appl. Catal.* **1995**, *132*, 127.
(163) Okuhara, T.; Kimura, M; Nakato, T. *Appl. Catal.* **1997**, *155*, L9.
(164) Timofeeva, M. N.; Maksimovskaya, R. I.; Paukshtis, E. A.; Kozhevnikov, I. V. *J. Mol. Catal. A: Chem.* **1995**, *102*, 73.
(165) Izumi, Y.; Ono, M.; Kitagawa, M.; Yoshida, M.; Urabe, K. *Microporous Materials* **1995**, *5*, 255.
(166) Soled, S.; Miseo, S.; McVicker, G. B.; Baumgartner, J. E.; Gates, W. E.; Gutierrez, A.; Paes, J. *Advanced Catalysis and Nanostructured Materials*; Moser, W. R., Ed.; Academic Press: New York, 1996; p 435.
(167) Soled, S.; Miseo, S.; McVicker, G.; Gates, W. E.; Gutierrez, A.; Paes, J. *Catal. Today* **1997**, *36*, 441.
(168) Mizuno, N.; Watanabe, T.; Mori, H.; Misono, M. *J. Catal.* **1990**, *123*, 157.
(169) Cavani, F.; Trifiro, F. *Catal. Today* **1997**, *36*, 431.
(170) Ai, M. In *Proc. 8th Intern. Congr. Catal., Berlin, 1984*; Verlag Chemie: Weinheim, 1985; Vol. 5, p 475.
(171) Centi, G.; Nieto, J. P.; Brükman, C. K.; Serwicka, E. M. *Appl. Catal.* **1989**, *46*, 197.
(172) Centi, G.; Lena, V.; Trifiro, F.; Ghoussoub, D.; Aïssi, C. F.; Guelton, M.; Bonnelle, J. P. *J. Chem. Soc., Faraday Trans.* **1990**, *86*, 2775.
(173) Centi, G.; Trifiro, F. *Catal. Sci. Technol.* **1991**, *1*, 225.
(174) Brükman, K.; Harber, J. In *Proc. 10th Intern. Congr. Catal., Budapest, 1992*; Elsevier: Budapest, 1993; p 742.
(175) Kringer, H.; Kirch, L. S. European Patent 0010902, 1979. Imai, H.; Nakatsukasa, M.; Aoshima, A. JP Patent (Jpn Kokai Tokkyo Koho) 62/132832. Imai, H.; Yamaguchi, T.; Sugiyama, M. JP Patent (Jpn Kokai Tokkyo Koho) 63/145249. Yamamatsu, S.; Yamaguchi, Y. JP Patent (Jpn Kokai Tokkyo Koho) 2/42033.
(176) Moffat, J. B. *Appl. Catal. A.* **1996**, *146*, 65.
(177) Mizuno, N.; Tateishi, T.; Iwamoto, M. *J. Chem. Soc., Chem. Commun.* **1994**, 1411.
(178) Mizuno, N.; Tateishi, T.; Iwamoto, M. *Appl. Catal. A* **1994**, *118*, L1.
(179) Mizuno, N.; Tateishi, M.; Iwamoto, M. *Appl. Catal. A: Gen.* **1995**, *128*, L165.
(180) Mizuno, N.; Suh, D.-J. *Appl. Catal. A: Gen.* **1996**, *146*, L249.
(181) Mizuno, N.; Tateishi, M.; Iwamoto, M. *J. Catal.* **1996**, *163*, 87.

(182) Mizuno, N.; Han, W.; Kudo, T.; Iwamoto, M. In *Proc. 11th Intern. Congr. Catal.*; Baltimore, 1996; p 1001.
(183) Mizuno, N.; Han, W.; Kudo, T. *J. Mol. Catal. A: Chem.* **1996**, *114*, 309.
(184) Mizuno, N.; Han, W.; Kudo, T. *Chem. Lett.* **1996**, 1121.
(185) Li, W.; Ueda, W. *Stud. Surf. Sci. Catal.* **1997**, *110*, 433.
(186) Ono, A.; Kubo, A.; Inumaru, K.; Misono, M. *73rd National Meeting of The Chemical Society of Japan*; Tokyo, 1997.
(187) Cavani, F.; Comuzzi, C.; Dolcetti, G.; Etienne, E.; Finke, R. G.; Selleri, G.; Trifiro, F.; Trovarelli, A. *J. Catal.* **1996**, *160*, 317.
(188) Comuzzi, C.; Dolcetti, G.; Trovarelli, A.; Cavani, F.; Trifiro, F.; Llorca, J.; Finke, R. G. *Catal. Lett.* **1996**, *36*, 75.
(189) Albonetti, S.; Cavani, F.; Trifiro, F.; Koutyrev, M. *Catal. Lett.* **1995**, *30*, 253.
(190) Cavani, F.; Koutyrev, M.; Trifiro, F. *Catal. Today* **1996**, *28*, 319.
(191) Otake, M.; Onoda, T. *J. Catal.* **1975**, *38*, 494.
(192) Tatibouet, J. M. *Appl. Catal. A* **1997**, *148*, 213.
(193) Ono, Y.; Taguchi, M.; Suzuki, S.; Baba, T. In *Catalysis by Acids and Bases*; Imelik, B., *et al.*, Eds.; Elsevier: Amsterdam, 1985; p 167. Ono, Y.; Baba, T.; Kanae, K.; Seo, S. G. *Nippon Kagaku Kaishi* **1988**, 985.
(194) Baba, T.; Ono, Y. *Appl. Catal.* **1989**, *55*, 301.
(195) Suzuki, S.; Kogai, K.; Ono, Y. *Chem. Lett.* **1984**, 699.
(196) Na, K.; Okuhara, T.; Misono, M. *J. Chem. Soc., Chem. Commun.* **1993**, 1422.
(197) Na, K.; Okuhara, T.; Misono, M. In *Catalytic Science and Technology II*; Izumi, Y., Arai, H., Iwamoto, M., Eds.; Kodansha: Tokyo; Elsevier: Amsterdam, 1995; p 245.
(198) Na, K.; Okuhara, T.; Misono, M. *J. Catal.* **1997**, *170*, 96.
(199) Stobbe-Kreemers, A. W.; Dielis, R. B.; Makkee, M.; Scholten, J. J. F. *J. Catal.* **1995**, *154*, 175. Stobbe-Kreemers, A. W.; van der Lans, G.; Makkee, M.; Scholten, J. J. F. *J. Catal.* **1995**, *154*, 187.
(200) Mizuno, N.; Ishige, T.; Seki, Y.; Misono, M.; Suh, D.-J.; Han, W.; Kudo, T. *Chem. Commun.* **1997**, 1295.
(201) Seki, Y.; Mizuno, N.; Misono, M. *Appl. Catal.* **1997**, *157*, L47.

CR960401Q